[redacted] SECURITY INFORMATION

Copy 237
RM E53G09

NACA

RESEARCH MEMORANDUM

EFFECT OF CIRCUMFERENTIAL LOCATION ON ANGLE OF ATTACK PERFORMANCE OF TWIN HALF-CONICAL SCOOP-TYPE INLETS MOUNTED SYMMETRICALLY ON THE RM-10 BODY OF REVOLUTION

By Alfred S. Valerino, Donald B. Pennington, and Donald J. Vargo

Lewis Flight Propulsion Laboratory
Cleveland, Ohio

[redacted]

NATIONAL ADVISORY COMMITTEE
FOR AERONAUTICS

WASHINGTON

September 9, 1953

[redacted]

NACA RM E53G09

[redacted]

NATIONAL ADVISORY COMMITTEE FOR AERONAUTICS

RESEARCH MEMORANDUM

EFFECT OF CIRCUMFERENTIAL LOCATION ON ANGLE OF ATTACK PERFORMANCE OF TWIN HALF-CONICAL SCOOP-TYPE INLETS MOUNTED SYMMETRICALLY ON THE RM-10 BODY OF REVOLUTION

By Alfred S. Valerino, Donald B. Pennington, and Donald J. Vargo

SUMMARY

An experimental investigation to determine the effects of circumferential inlet location on the performance of twin half-conical scoop-type inlets with and without boundary-layer removal was conducted at Mach numbers 1.49, 1.79, and 1.99 through an angle-of-attack range from 0° to 10°. Twin inlets were mounted symmetrically on the NACA RM-10 body of revolution at four circumferential locations at the station of maximum diameter.

Results indicated that for positive angles of attack, higher pressure recovery performance was obtained with the inlets mounted on the fuselage lower quadrants than on the upper quadrants. Increasing the amount of boundary-layer removal from zero to complete removal resulted in a significant increase in critical pressure recovery as well as in model minimum drag. These increases when applied to a complete missile configuration indicated a substantial gain in the net propulsive thrust of the missile over the configuration without boundary-layer removal. At zero angle of attack, an unfavorable interference drag caused the minimum drag coefficients of the configurations having inlets at the 45° positions of the fuselage to be higher than those of the diametrically opposite inlet configurations.

INTRODUCTION

Much of the available data on the performance characteristics of a scoop-type side inlet have been obtained from investigations of inlets mounted either on flat plates or at fixed positions on a specific fuselage. Because of the potential cross-flow effects and the variable boundary-layer thickness along the periphery of a fuselage at angles of attack, significant effects on the angle-of-attack performance of an inlet could result from changes in its peripheral location.

[redacted]

[redacted]

In order to evaluate the influence of circumferential location on the angle of attack performance of an inlet, an investigation was conducted in the NACA Lewis 8- by 6-foot supersonic tunnel. A concurrent investigation which was conducted at the Langley laboratory is reported in reference 1.

Twin half-conical scoop-type inlets, mounted symmetrically at four circumferential locations at the station of maximum diameter of the NACA RM-10 body of revolution (ref. 2), were investigated at Mach numbers of 1.99, 1.79, and 1.49 through an angle of attack range from 0° to 10° with and without boundary-layer removal ahead of the inlets. Boundary-layer removal was accomplished by employing 16° bypass wedges of heights equal to and twice the boundary-layer thickness at zero angle of attack. The Reynolds number based on the model length ahead of the inlets was approximately 17×10^6.

SYMBOLS

The following symbols are used in this report:

A	area
C_D	total external drag coefficient based on maximum frontal area of each configuration
C_D'	total external drag coefficient based on maximum frontal area of configuration with zero boundary-layer removal
C_L	external lift coefficient based on maximum frontal area of each configuration
C_M	coefficient of external moments about station 45 of RM-10 body, based on maximum frontal area of each configuration and overall length of RM-10 body
D	external drag force
h	height of wedge spacer
h/δ	boundary-layer parameter
L	external lift force
L/D	lift-drag ratio
M	Mach number
m	mass flow
P	total pressure

P'	pitot pressure
x	distance from cowl lip
y	distance from center line of fuselage to center line of duct at duct exit station
α	angle of attack
δ	boundary-layer thickness
θ	inlet circumferential location with respect to bottom of RM-10 body

Subscripts:

c	projected inlet capture area
cr	critical
L	local
l	lip
0	free stream
2	diffuser discharge station, 17.5

APPARATUS AND PROCEDURE

A photograph and a schematic diagram of the RM-10 twin-scoop inlet configuration are presented in figures 1 and 2. Twin inlets located symmetrically at four locations around the circumference of the RM-10 body at station 45 were investigated. The inlet positions were: diametrically opposite at top and bottom of the fuselage ($\theta = 0^\circ$ and 180°, respectively), diametrically opposite in the horizontal plane ($\theta = 90^\circ$ and 270°), at the 45° positions of the fuselage upper quadrants ($\theta = 135^\circ$ and 225°), and at the 45° positions of the fuselage lower quadrants ($\theta = 45^\circ$ and 315°).

Details of the inlets are presented in figure 3. The inlets, which had a total capture area of 21.7 percent of the basic fuselage frontal area, were designed so that the oblique shock generated by the 25° half-cone centerbodies would fall slightly ahead of the cowl lip for the local Mach number ahead of the inlets corresponding to a free-stream Mach number of 2.0. Swept-back splitter plates of 78° included angle having their apexes alined with the tips of the cones were employed. The floors of the inlets were designed to be parallel to the circular surface of the RM-10 body of revolution. The resulting sharp corners [redacted]

at the cowl and splitter plate junctions were eliminated by use of internal fillets. The corner fillets were tapered from zero radius at the lip station to a 1/4-inch radius at inlet station 1 and remained constant to inlet station 24.5. The cowling cross section was gradually changed from a nearly sector-shaped section of 1.33-inch radius at the lip station to a circular cross section of 1.41-inch radius at the inlet station 24.5. The area variation of the inlets is presented in figure 4.

The boundary-layer air was bypassed around the inlets by positioning them radially outward from the body and inserting the wedge-shaped spacers of 16° included angle between the floors of the inlets and the fuselage surface of the RM-10 body (see photograph, fig. 5). Wedge spacers of 0.375-inch and 0.750-inch heights were employed to obtain the boundary-layer parameters h/δ of 1.0 and 2.0, respectively, as determined by preliminary flow surveys of the boundary layer at zero angle of attack. These wedge spacers were alined with the tips of the swept-back splitter plates (fig. 5). The thicknesses of the 0.375-inch and 0.750-inch bypass wedges were increased downstream of the lip station to maintain the alinement shown in the table of figure 2. The condition of zero boundary-layer removal was obtained by placing the inlets directly on the RM-10 body. With the zero boundary-layer-removal configuration, spacers were used at the rear of the RM-10 body for alinement purposes.

A preliminary survey of the flow conditions at the inlet lip (station 45 of the RM-10 body) was conducted to determine the boundary-layer thickness around the circumference of the RM-10 body. The results of this survey are presented as contour maps in figures 6 and 7. Local to free-stream total-pressure ratios at zero angle of attack are presented in figure 6. The boundary-layer thickness δ at zero angle of attack was estimated to be 0.375 inch at free-stream Mach numbers of 1.99 and 1.49. The local Mach number at the lip station, corresponding to the free-stream Mach number of 1.99, was approximately 2.06. Angle of attack results are presented in figure 7 as contour maps of local pitot to free-stream total-pressure ratios. As would be expected, the boundary-layer thickness δ, represented by the dashed lines, increased along the upper surface and decreased along the lower surface of the RM-10 body as the angle of attack was increased. The lobes, attributed to separation as reported in references 2 and 3, were observed at 8° and 10° angle of attack. However, small effects of separation were found at 4° angle of attack. The inlet positions for the $h = 0.375$ inch configurations are superimposed on the figures to indicate the amount of boundary layer entering the inlets.

The mass flow through the inlets was varied by means of remotely controlled plugs attached to the model sting. A three component internal strain gage balance, located at station 45, was used to measure the axial forces on the model but not the forces acting on the plugs. Moments and normal forces were also measured by the strain gage balance.

Pressure instrumentation consisting of 18 total-pressure tubes and 4 wall static orifices in one inlet and 4 wall static orifices in the

other inlet was located at inlet station 17.5 The average total pressure at inlet station 17.5 was determined by an area weighting method and was used to calculate the mass flows based on a choked exit at the control plugs. The mass flows presented are those obtained from the inlet having total-pressure instrumentation. Eight static orifices located on the base of the configuration were used to determine an average base pressure.

DISCUSSION OF RESULTS

The mass flow, pressure recovery, and drag characteristics of the inlet configurations are presented for free-stream Mach numbers of 1.99, 1.79, and 1.49 in figures 8 to 11. The mass-flow ratio is defined as the ratio of the mass flow entering the inlet to the mass flow passing through a free-stream tube area equal to the projected capture area of the inlet. The drag is defined as the strain gage balance force minus the thrust developed minus the base force. The internal thrust is a result of the change of momentum of the air passing through the inlet from free stream to inlet station 24.5. Base forces were computed from the base area and the average base pressures. Since the configurations investigated did not include wings or an afterbody, the drag coefficients at angles of attack are presented primarily to indicate the magnitude of the additive drags associated with the inlets. The drag characteristics of the configuration with inlets having different mass flows at angles of attack (inlets at $\theta = 0^\circ$ and 180°) are presented as a function of diffuser discharge Mach number M_2.

For a fixed wedge height configuration at all Mach numbers, scatter in mass-flow - pressure recovery characteristics was obtained with changes in inlet circumferential location (see figs. 8 to 11). This scatter, which could not be explained, was predominant with the h = 0.750 inch configuration. The mass flow, pressure recovery, and drag characteristics were plotted against diffuser discharge Mach number M_2 as an aid in determining the critical values shown in figures 8 to 11.

The mass-flow range for stable operation at 0° angle of attack was approximately 11 to 17 percent at a free-stream Mach number of 1.99, regardless of the wedge height. At angles of attack, the stable range was generally increased as the wedge height was increased. Largest stability range at angles of attack was obtained when the inlets were located at either the bottom or top positions ($\theta = 0^\circ$ and 180°).

Zero Angle of Attack

The effects of the boundary-layer bypass wedge height on the critical values of the characteristics of the inlet configurations at zero angle of attack are summarized in figure 12. Since the only boundary-layer parameters h/δ investigated were 0, 1.0, and 2.0, the exact trends of the curves are not known and therefore dashed curves are used.

With the zero boundary-layer-removal configurations, extremely low pressure recoveries were obtained. As h/δ was increased to 1.0, substantial increases in critical pressure recoveries occurred. For example, at a Mach number of 1.99, an improvement of 27 percent of free-stream total pressure was observed. This increase in critical pressure recovery corresponds to approximately a 32 percent increase in the thrust of a turbojet engine. Insignificant gains in critical pressure recovery were realized at a Mach number of 1.99 as h/δ was increased from 1.0 to 2.0. Each increase in h/δ, however, resulted in increases in the critical mass-flow ratios.

Two drag coefficients are presented in figure 12; C_D, which is based on the maximum cross sectional area of each configuration, and C_D', which is based on the maximum cross sectional area of the $h = 0$ configuration. Each increase in h/δ resulted in increased drag coefficient C_D for all inlet configurations with the exception of those with inlets in the 45° positions. For these configurations, the drag coefficient remained essentially constant as h/δ was increased from 1.0 to 2.0. Because of an unfavorable interference drag, the drag coefficients C_D of the configurations with inlets at the 45° positions of the fuselage were higher than those of the configurations having inlets diametrically opposite. The largest interference drag was obtained with the $h/\delta = 1.0$ configurations. At a Mach number of 1.99 and $h/\delta = 1.0$, the minimum drag coefficient C_D of the configurations having inlets at the 45° positions was approximately 11 percent higher than those of the diametrically opposite inlet configurations.

The net drag penalty associated with increasing the bypass wedge height, represented by the C_D' plot, increased with increasing h/δ regardless of the inlet location. This would be expected because of the increase in configuration frontal area. At a Mach number of 1.99, for the configurations having inlets diametrically opposite ($\theta = 0°$ and 180° and $\theta = 90°$ and 270°), the model minimum drag of the $h/\delta = 1.0$ configuration was approximately 25 percent higher than that of the $h/\delta = 0$ configuration. Increasing h/δ from 1.0 to 2.0 resulted in a 12 percent increase in the model minimum drag over that of the $h/\delta = 1.0$ configuration. The 25 percent rise in minimum drag of the configurations having diametrically opposite inlets, due to complete boundary-layer removal, corresponds to approximately a 7 percent increase in the minimum cruise drag of a typical missile such as reported in reference 4. At Mach number 1.99, with the configurations having inlets mounted at the 45° positions of the fuselage ($\theta = 135°$ and 225° and $\theta = 45°$ and 315°), the model minimum drag of the $h/\delta = 1.0$ configuration was 33 percent higher than that of the $h/\delta = 0$ configuration. As the h/δ was increased to 2.0, the model minimum drag penalty was 4 percent of the minimum drag of the $h/\delta = 1.0$ configuration.

Angle of Attack

The effect of angle of attack on the critical pressure recoveries of the inlet configurations is presented in figure 13. These data will be discussed according to inlet position.

Inlet mounted at $\theta = 0^\circ$. - At each Mach number and for each wedge height configuration, the highest pressure recovery performance throughout the angle of attack range was obtained with the inlet located at the bottom of the fuselage ($\theta = 0^\circ$). With the $h = 0$ configuration, the critical pressure recovery increased with increasing angle of attack primarily because of the decrease in boundary-layer thickness. Although substantial increases in critical pressure recovery resulted with increasing angle of attack, the magnitudes of the critical pressure recoveries were still significantly lower than those obtained at zero angle of attack with the configurations utilizing boundary-layer removal. The critical pressure recoveries of the $h = 0.375$ and $h = 0.750$ inch configurations remained relatively constant with increasing angle of attack because the inlets at $\theta = 0^\circ$ were always operating at h/δ greater than unity (see fig. 7).

Inlets mounted at $\theta = 45^\circ$ and 315°. - The second highest pressure recovery performance was obtained when the inlets were located at the 45° positions of the fuselage lower quadrants. With the $h = 0$ configuration, the critical pressure recoveries increased as the angle of attack was increased to 3° and then remained essentially constant. With the configurations utilizing boundary-layer removal, the critical pressure recoveries decreased with increasing angle of attack. However, the losses in the critical pressure recoveries of the $h = 0.750$ inch configuration at the higher angles of attack (6° and 10°) were approximately one-half those obtained with the $h = 0.375$ inch configuration. These angle of attack losses were probably due to the cross flow effects. Thus significant pressure recovery losses at angles of attack might be reduced by moving the inlets outward from the body flow field.

Inlets mounted at $\theta = 90^\circ$ and 270° and at $\theta = 135^\circ$ and 225°. - Large drops in critical pressure recoveries with increasing angle of attack resulted with all configurations having inlets at $\theta = 90^\circ$ and 270° and at $\theta = 135^\circ$ and 225°. However, gains in the critical pressure recoveries at angles of attack were realized with each increase in the amount of boundary layer removed.

It should be noted that if the inlets located at the upper and lower 45° positions and in the horizontal plane were canted with respect to the fuselage, the large losses in the pressure recoveries suffered at angles of attack could be decreased.

Inlet mounted at $\theta = 180^\circ$. - With the inlet located at the top of the fuselage, significant losses in critical pressure recoveries resulted up to 3° angle of attack with the $h = 0$ configuration and up to 6° angle of attack with the $h = 0.375$ and 0.750 inch configurations. As the angle of attack was further increased, the performance of the configurations was improved by the presence of the body "separation lobes" which allowed more high-energy air to enter the inlets (see fig. 7). At 10° angle of attack, the critical pressure recoveries of the $h = 0$ configuration were nearly equal to or slightly greater than those at 0° angle of attack. However, the critical pressure recoveries remained low, never reaching the magnitude of the critical pressure recoveries of the configurations operating with boundary-layer removal and at 0° angle of attack.

The effects of angle of attack on the external lift coefficient and lift-drag ratio of each inlet configuration are presented in figures 14 and 15. Although the absolute values of the lift coefficients and lift-drag ratios presented are not applicable for a complete missile configuration, the plots are indicative of the trend that can be expected when the inlet circumferential location is changed. The external lift is defined as the difference between the measured value and the computed value of the internal lift component of the momentum of the inlet mass flow. The lift coefficients were essentially independent of mass flow and boundary-layer wedge height. The highest lift coefficients at angles of attack were obtained with the configuration having inlets located at $\theta = 90^\circ$ and 270°. In order to take advantage of this high lift, however, the pressure recoveries of inlets located at $\theta = 90^\circ$ and 270° would have to be less sensitive to changes in angles of attack than these inlets investigated. The configuration with inlets at $\theta = 0^\circ$ and 180° (top and bottom) had the lowest lift coefficients at angles of attack. Similarly, the highest and lowest lift-drag ratios at critical mass flows (fig. 5) of the $h = 0.375$ inch configuration were obtained with the inlets located at $\theta = 90^\circ$ and 270° and at $\theta = 0^\circ$ and 180°, respectively. There was very little to be gained in lift-drag ratios by selecting one configuration with inlets at the 45° positions over the other.

The effect of angle of attack on the external moment coefficients at critical mass flows of the $h = 0.375$ inch configuration is presented in figure 16. The external moments presented were computed by subtracting the moments due to the base forces and internal thrusts from the measured moments at station 45 of the RM-10 body.

It was found that the external moment coefficients of the configuration having inlets at $\theta = 0^\circ$ and 180° remained essentially constant with mass flow throughout the angle of attack range. With the inlets mounted at $\theta = 90^\circ$ and 270° and at $\theta = 135^\circ$ and 225°, the external moment coefficient generally decreased with decreasing mass flows. For

the configuration having inlets mounted at $\theta = 45^\circ$ and 315°, the external moments at all angles of attack except 10° increased slightly with decreasing mass flows. At 10° angle of attack, the moments decreased with decreasing mass flows.

SUMMARY OF RESULTS

The following results were obtained from an investigation to determine the effects of inlet circumferential location on the angle of attack performance of twin half-conical scoop-type inlets with and without boundary-layer removal mounted at four circumferential positions at the station of maximum diameter of the NACA RM-10 body of revolution:

1. The highest pressure recovery performance resulted with the inlet located at the bottom of the fuselage. This location was the only inlet position not adversely affected by increases in angle of attack. The critical pressure recoveries of the inlets utilizing boundary-layer removal remained essentially constant with increasing angle of attack. With the zero boundary-layer-removal configuration, the critical pressure recoveries, which were extremely low, increased substantially with increasing angle of attack but never reached the zero angle of attack critical pressure recoveries of the inlets utilizing boundary-layer removal.

2. The second highest pressure recovery performance was obtained with the twin inlets located at the 45° positions of the fuselage lower quadrants. Moving the inlets to the top of the fuselage resulted in progressively larger angle of attack losses in the critical pressure recoveries except for the inlet mounted at the top of the fuselage. For this exception, the pressure recovery losses were reduced at the higher angles of attack.

3. As the boundary-layer bypass wedge height was increased from 0 to the value equal to the boundary-layer thickness at zero angle of attack, significant gains in pressure recovery were obtained at any angle of attack with all inlet configurations. Increasing the wedge height from the boundary-layer thickness to twice the boundary-layer thickness resulted in substantial improvements in the angle of attack performance of the inlets located in the upper quadrants of the fuselage. With the inlets located at the 45° positions of the fuselage lower quadrants, substantial gains were evident only at the higher angles of attack (6° and 10°). For the inlet at the bottom of the fuselage, no significant gains resulted at Mach numbers of 1.99 and 1.49.

[redacted]

4. At a Mach number of 1.99 and zero angle of attack, increasing the bypass wedge height from 0 to the boundary-layer thickness resulted in a gain in critical pressure recovery equal to 27 percent of free-stream total pressure. This increase corresponds to approximately a 32 percent increase in the thrust of a turbojet engine. Accompanying this increase in critical pressure recovery was a 25 percent increase in model minimum drag for the configurations having inlets mounted diametrically opposite. This model drag penalty would correspond to approximately a 7 percent increase in the cruise drag of a missile configuration. When the inlets were located at the 45° position of the fuselage upper and lower quadrants, the model configuration drag was increased 33 percent because of complete boundary-layer removal. Increasing the wedge height from 1 to 2 boundary-layer thicknesses resulted in insignificant gains in the zero angle of attack critical pressure recovery and 12 percent and 4 percent drag penalty for the configurations having diametrically opposite inlets and inlets at the 45° positions, respectively.

5. Higher model minimum drag coefficients at zero angle of attack were obtained with the configurations having inlets mounted at the 45° positions than with the configurations having inlets mounted diametrically opposite.

Lewis Flight Propulsion Laboratory
National Advisory Committee for Aeronautics
Cleveland, Ohio, July 21, 1953

REFERENCES

1. Hasel, Lowell E., Lankford, John L., and Robins, A. W.: Investigation of a Half-Conical Scoop Inlet Mounted at Five Alternate Circumferential Locations Around a Circular Fuselage. Pressure-Recovery Results at a Mach Number of 2.01. NACA RM L53D30b, 1953.

2. Luidens, Roger W., and Simon, Paul C.: Aerodynamic Characteristics of NACA RM-10 Missile in 8- by 6-Foot Supersonic Wind Tunnel at Mach Numbers from 1.49 to 1.98. I - Presentation and Analysis of Pressure Measurements (Stabilizing Fins Removed). NACA RM E50D10, 1950.

3. Allen, H. Julian, and Perkins, Edward W.: Characteristics of Flow over Inclined Bodies of Revolution. NACA RM A50L07, 1951.

4. Fradenburgh, Evan A., and Campbell, Robert C.: Characteristics of a Canard-Type Missile Configuration with an Underslung Scoop Inlet at Mach Numbers from 1.5 to 2.0. NACA RM E52J22, 1953.

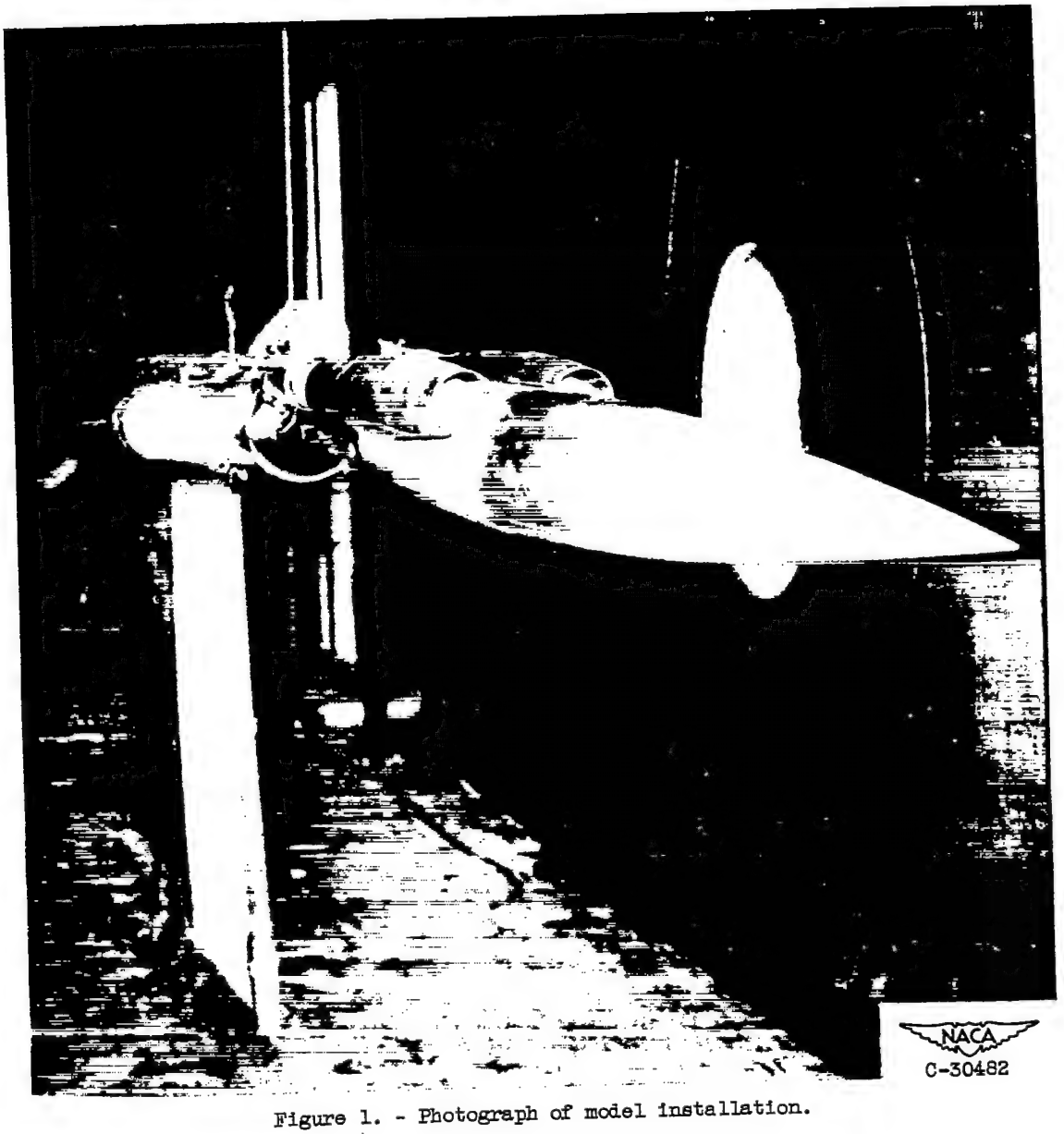

Figure 1. - Photograph of model installation.

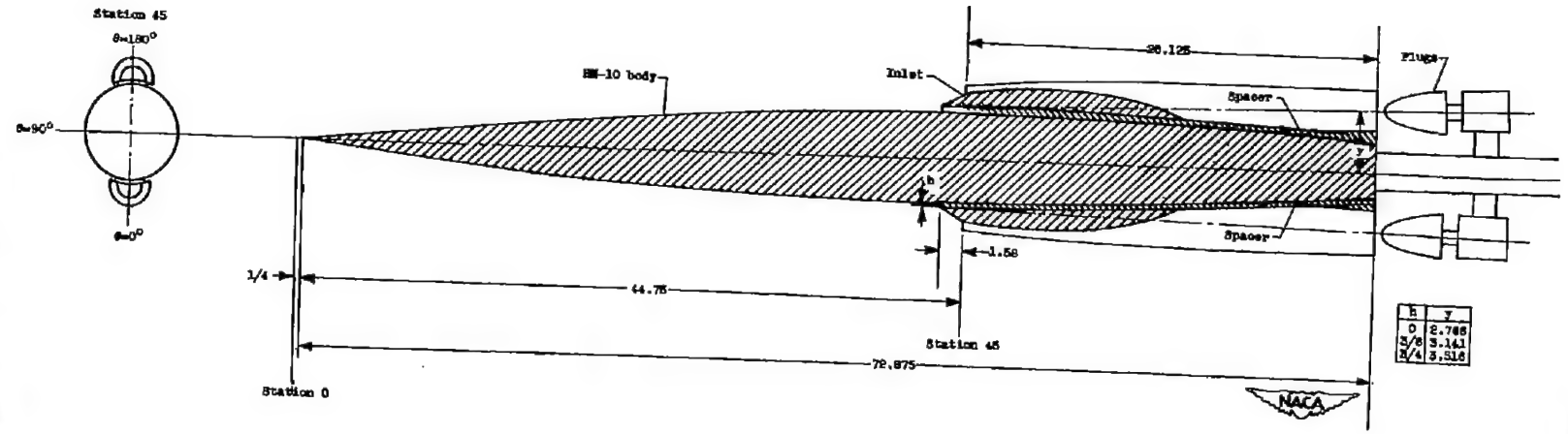

Figure 2. - Schematic diagram of twin scoop inlets mounted on RM-10 body. (All dimensions are in inches.)

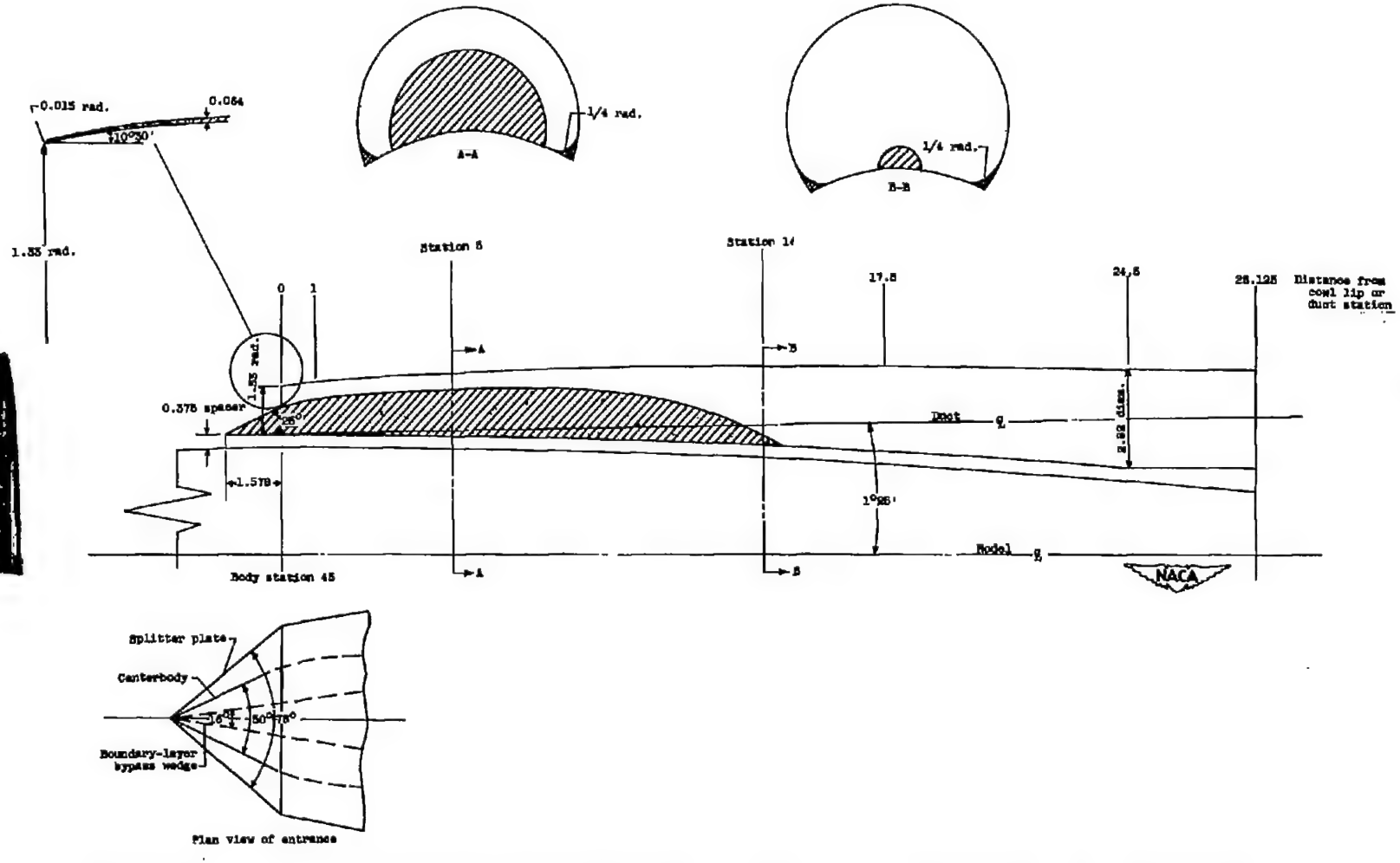

Figure 3. - Schematic diagram of inlet. (All dimensions are in inches.)

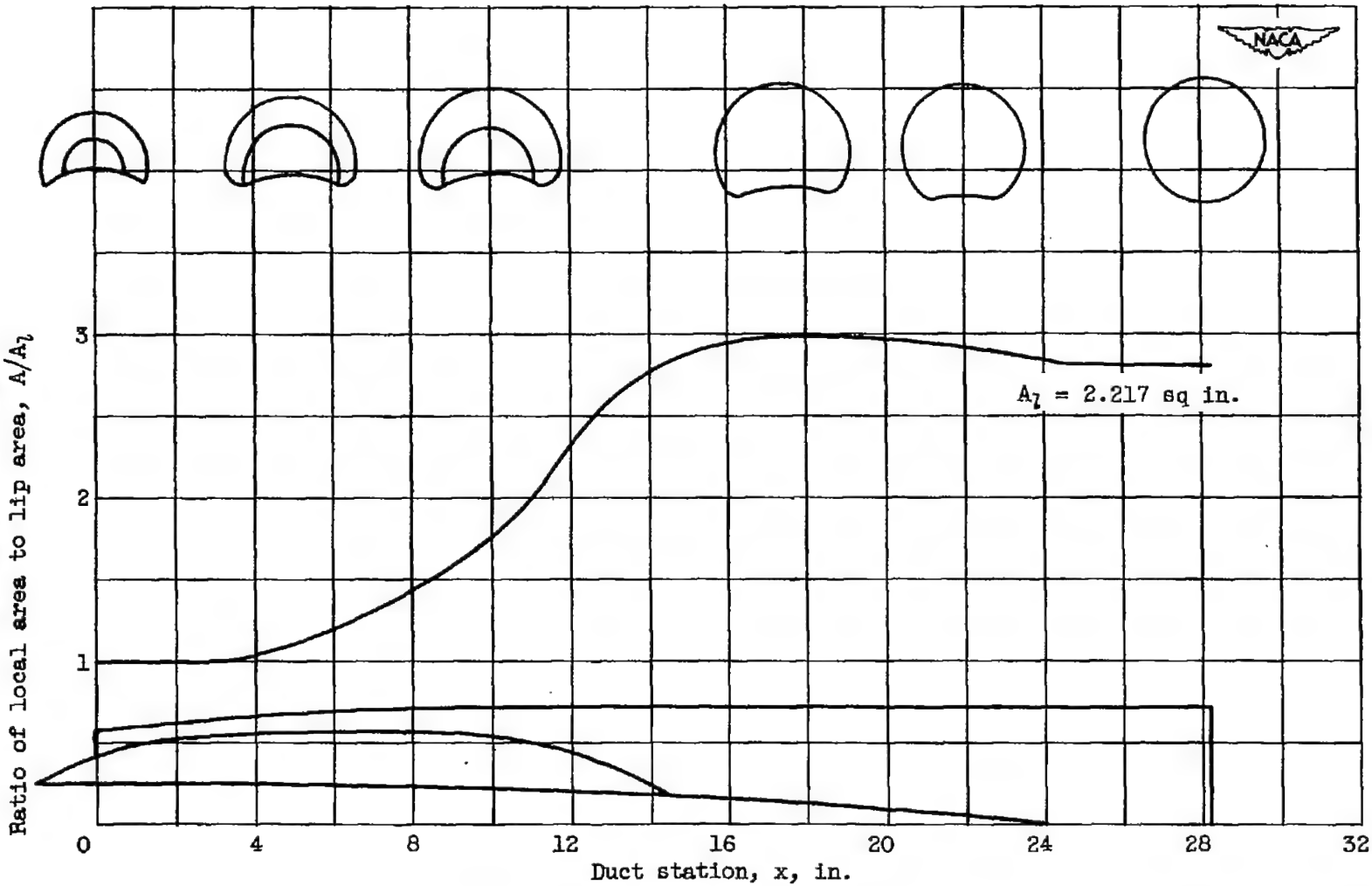

Figure 4. - Area variation of inlet.

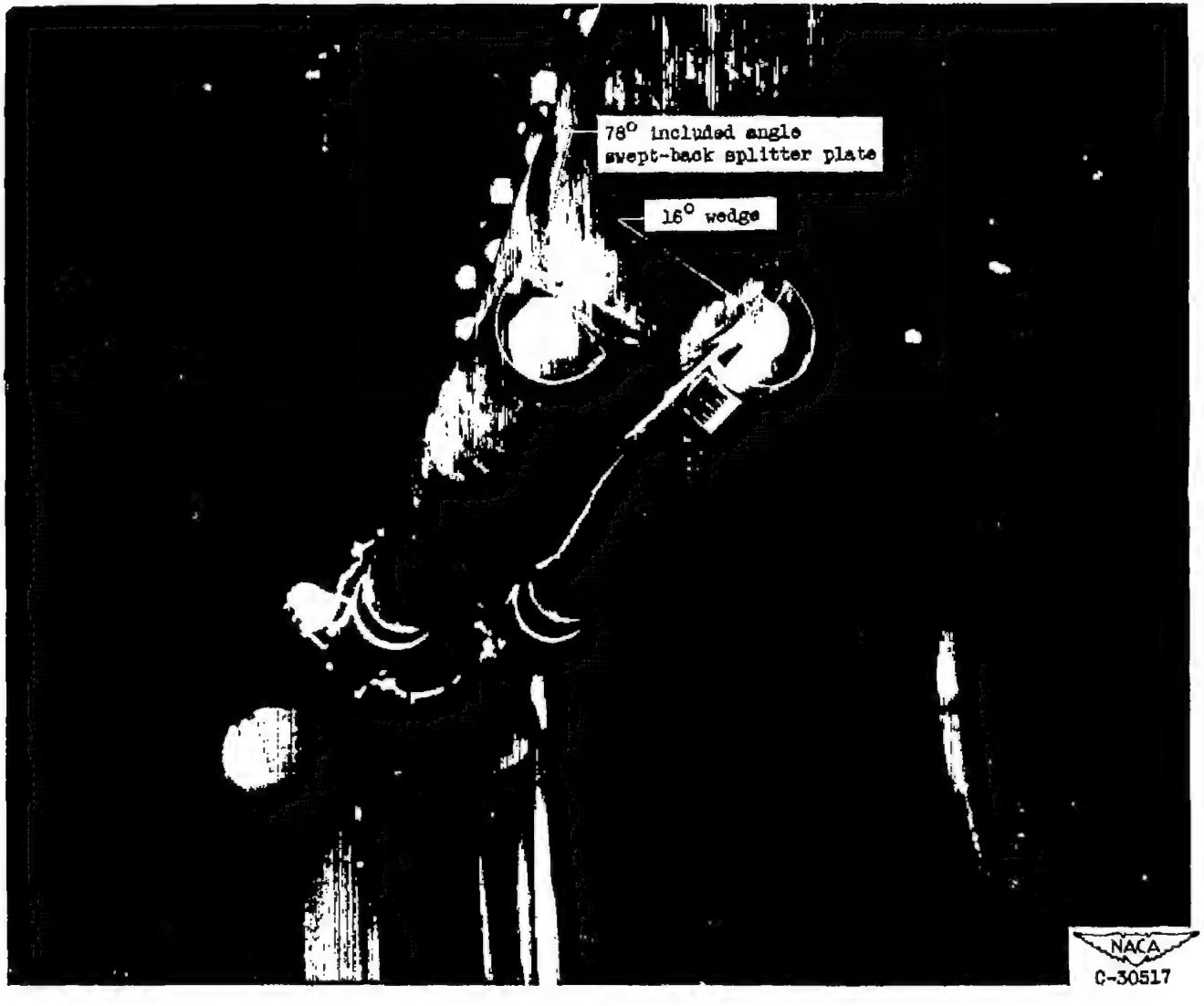

Figure 5. - Photograph of twin inlets mounted at $\theta = 45^{\circ}$ and 315°.

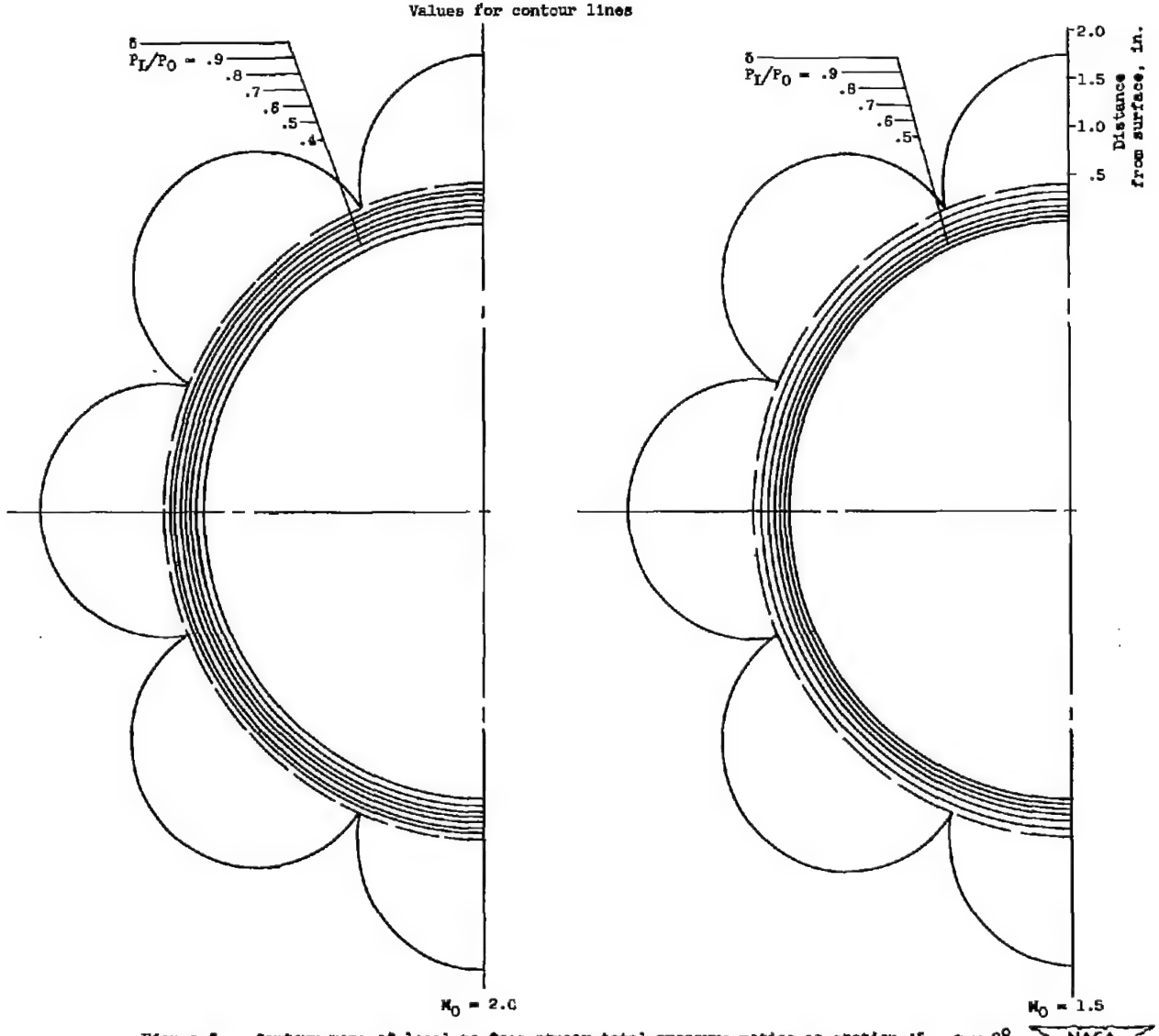

Figure 6. - Contour maps of local to free-stream total-pressure ratios at station 45. $\alpha = 0°$.

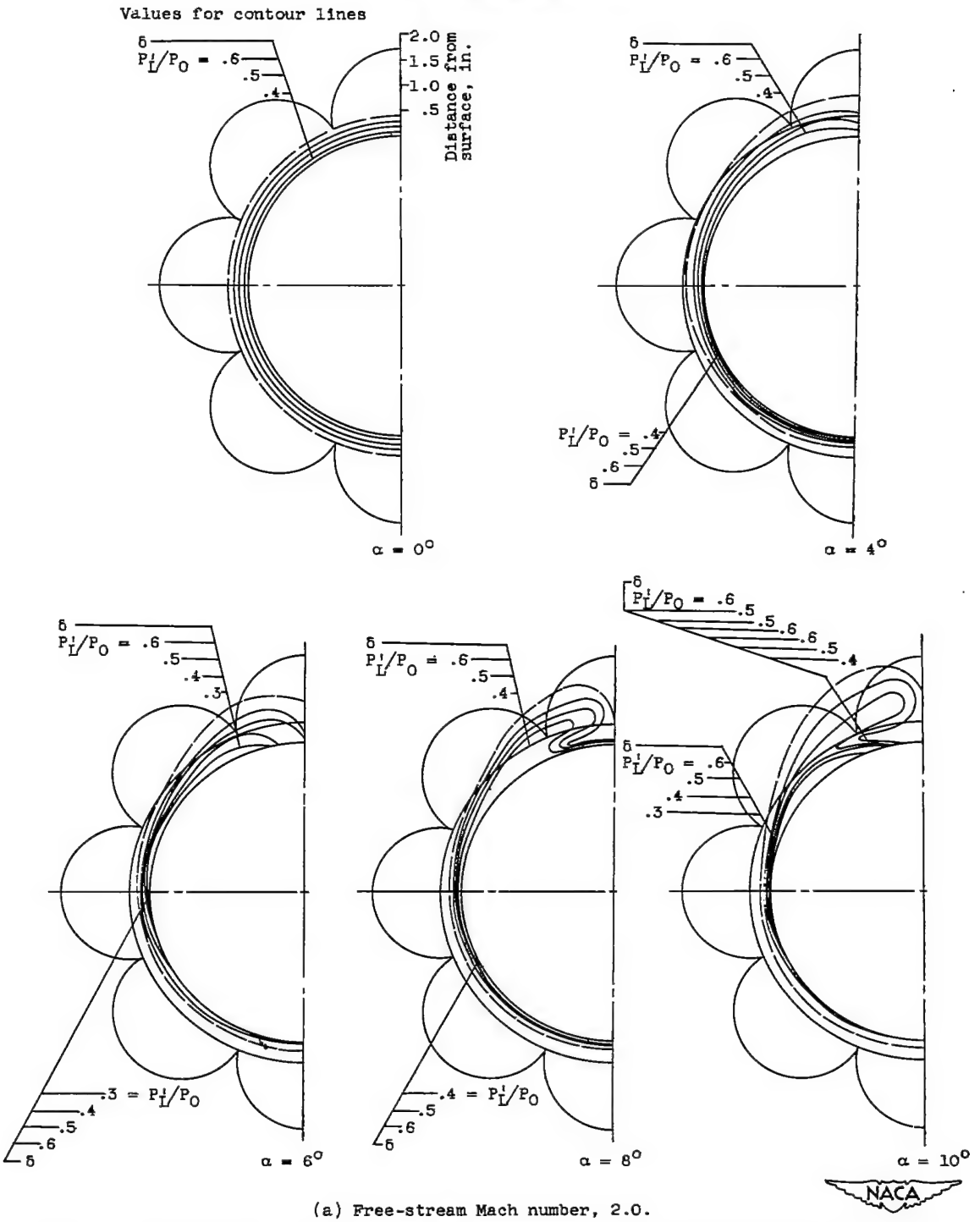

(a) Free-stream Mach number, 2.0.

Figure 7. - Contour maps of local pitot to free-stream total-pressure ratios at station 45.

[redacted]

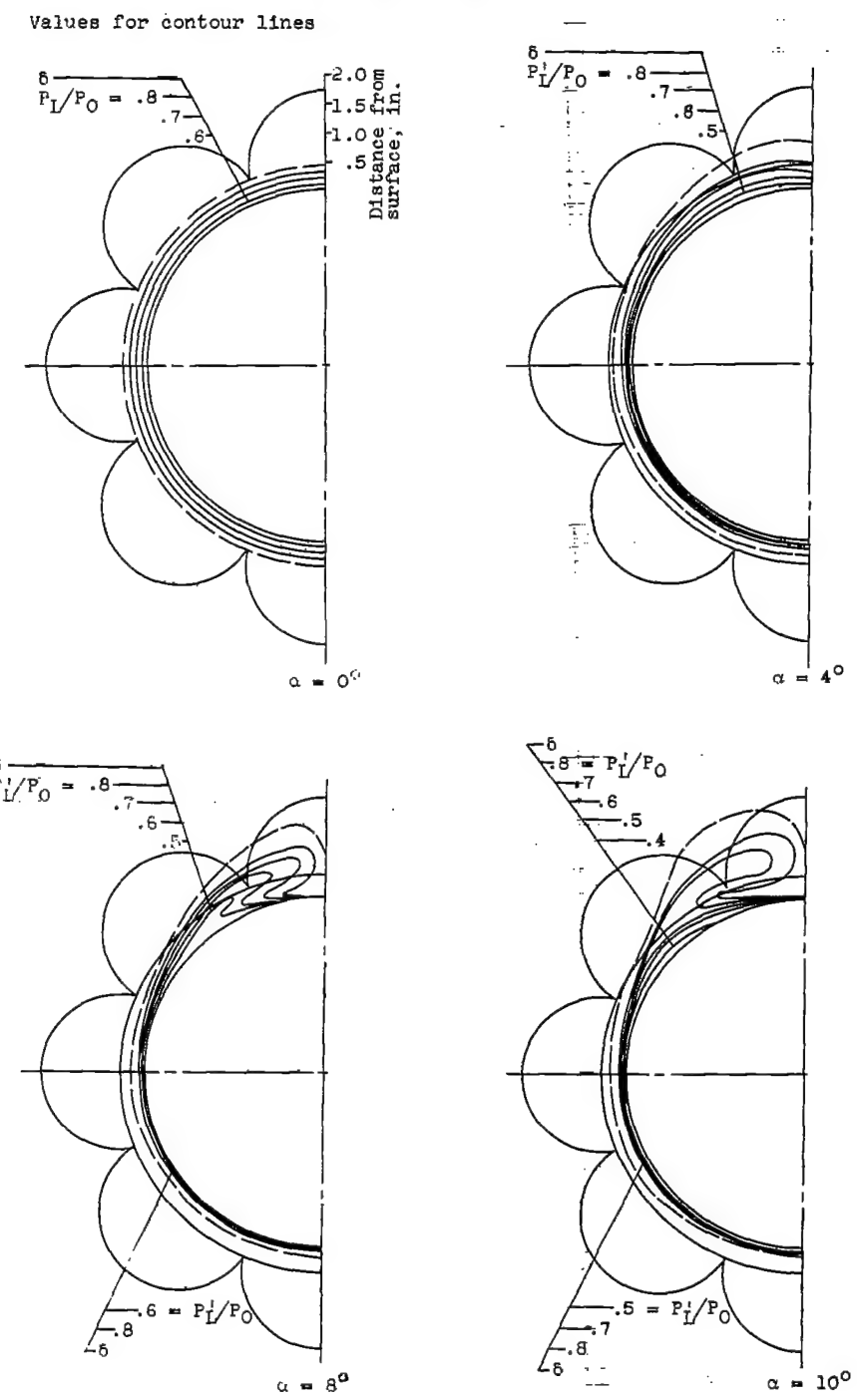

(b) Free-stream Mach number, 1.5.

Figure 7. - Concluded. Contour maps of local pitot to free-stream total-pressure ratios at station 45.

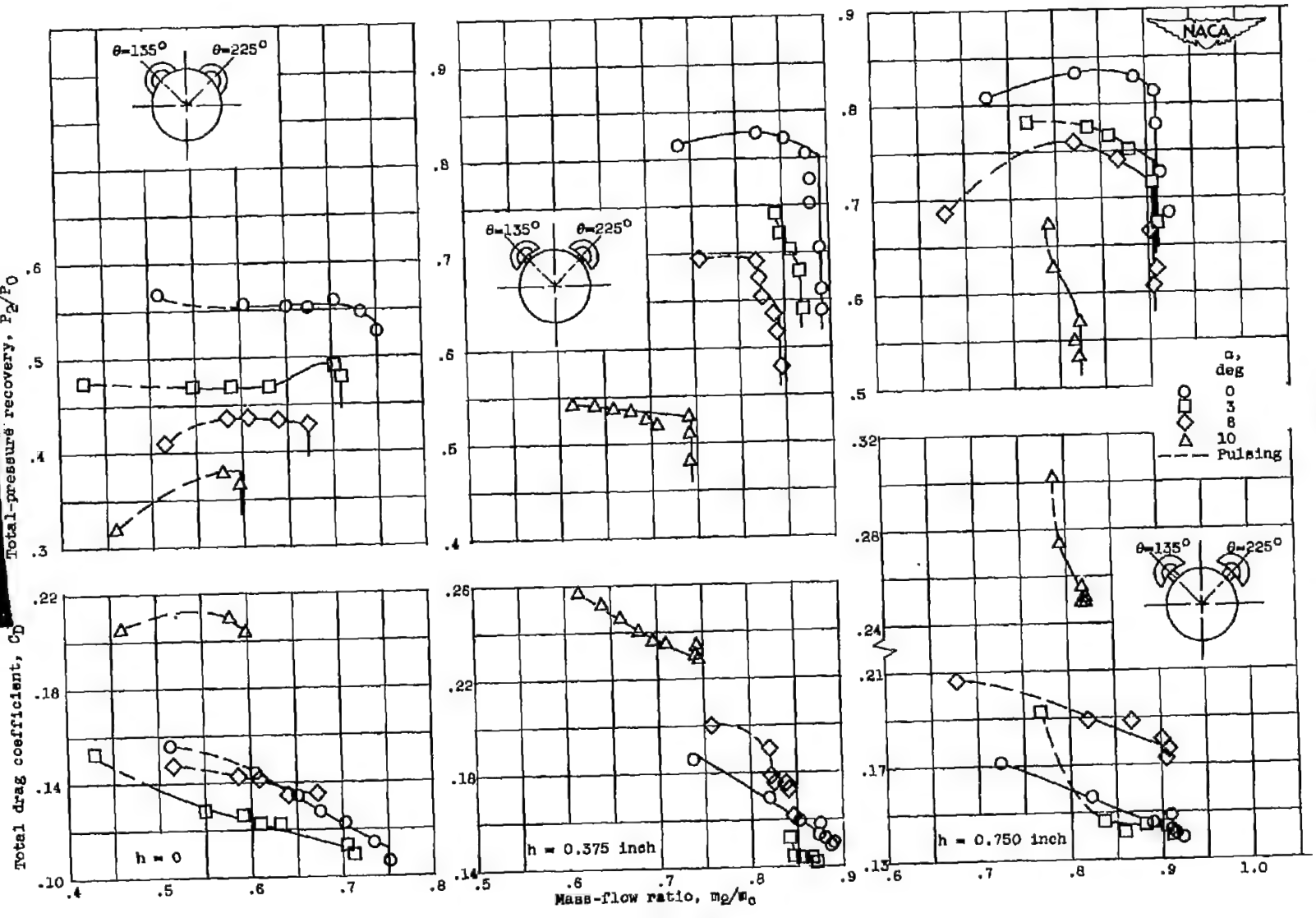

(a) Free-stream Mach number, 1.99.

Figure 8. - Angle of attack characteristics of RM-10 inlet configuration. θ = 135° and 225°.

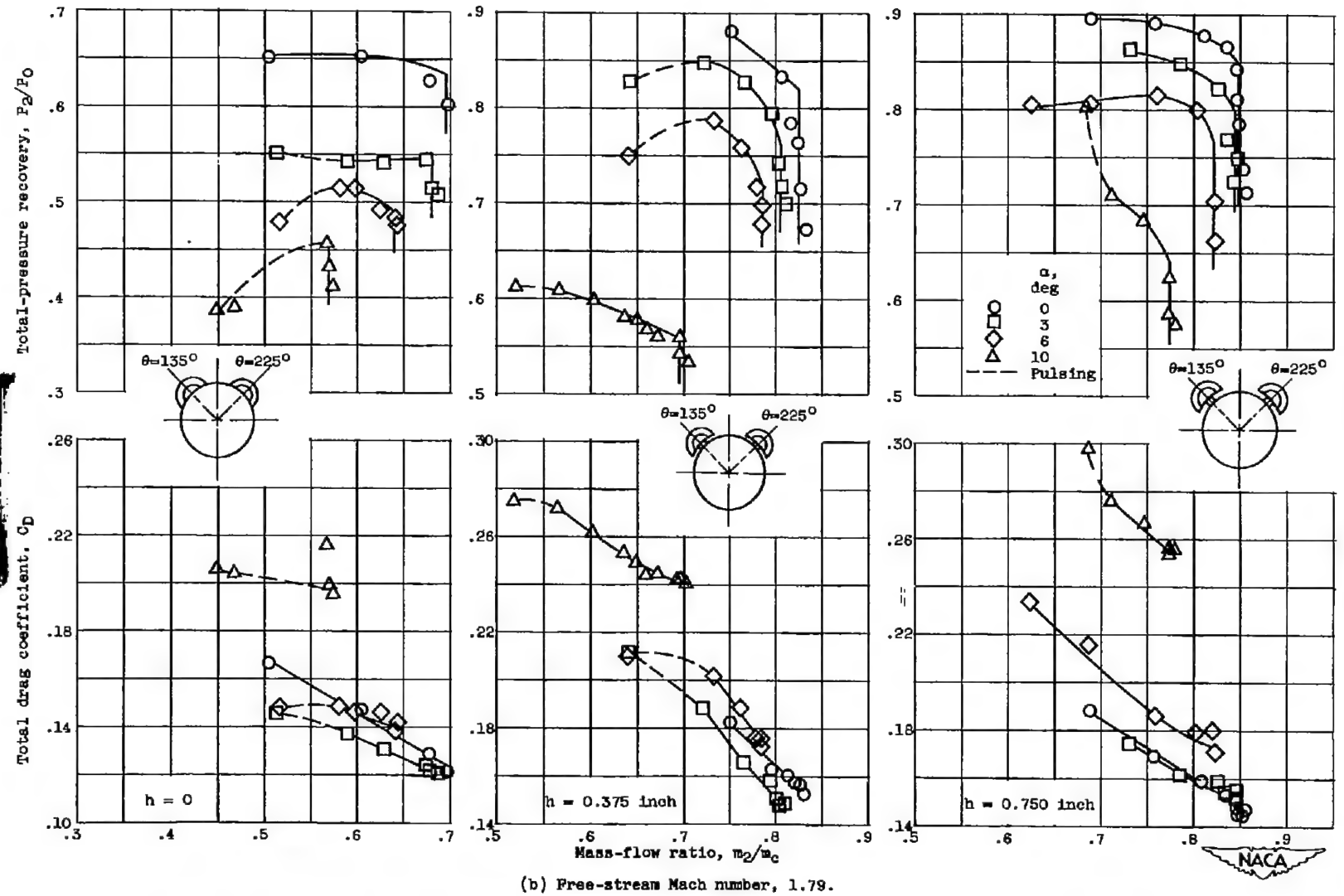

(b) Free-stream Mach number, 1.79.

Figure 8. - Continued. Angle of attack characteristics of RM-10 inlet configuration. θ = 135° and 225°.

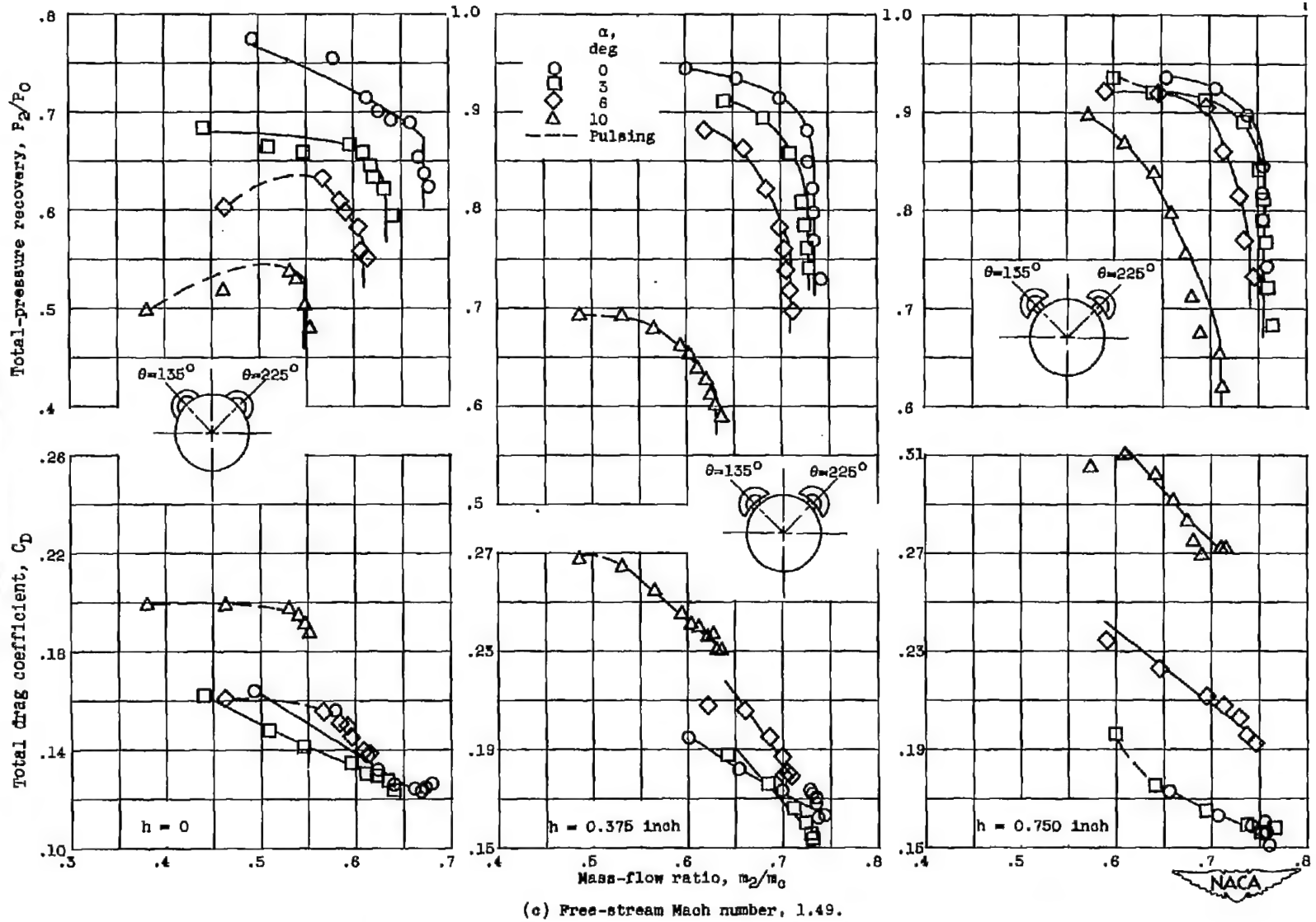

(c) Free-stream Mach number, 1.49.

Figure 8. - Concluded. Angle of attack characteristics of RM-10 inlet configuration. θ = 135° and 225°.

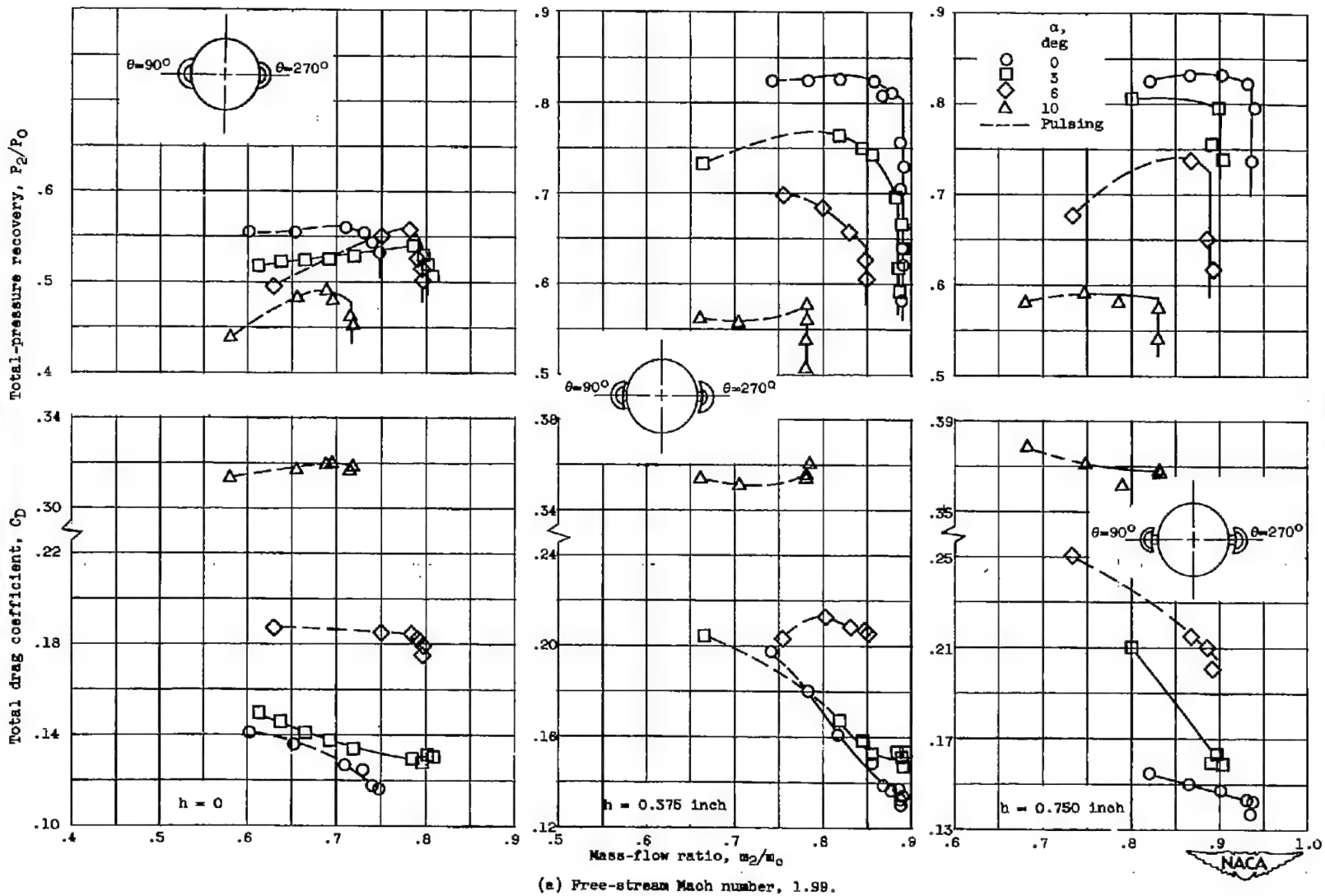

(a) Free-stream Mach number, 1.99.

Figure 9. - Angle of attack characteristics of RM-10 inlet configuration. ϕ = 90° and 270°.

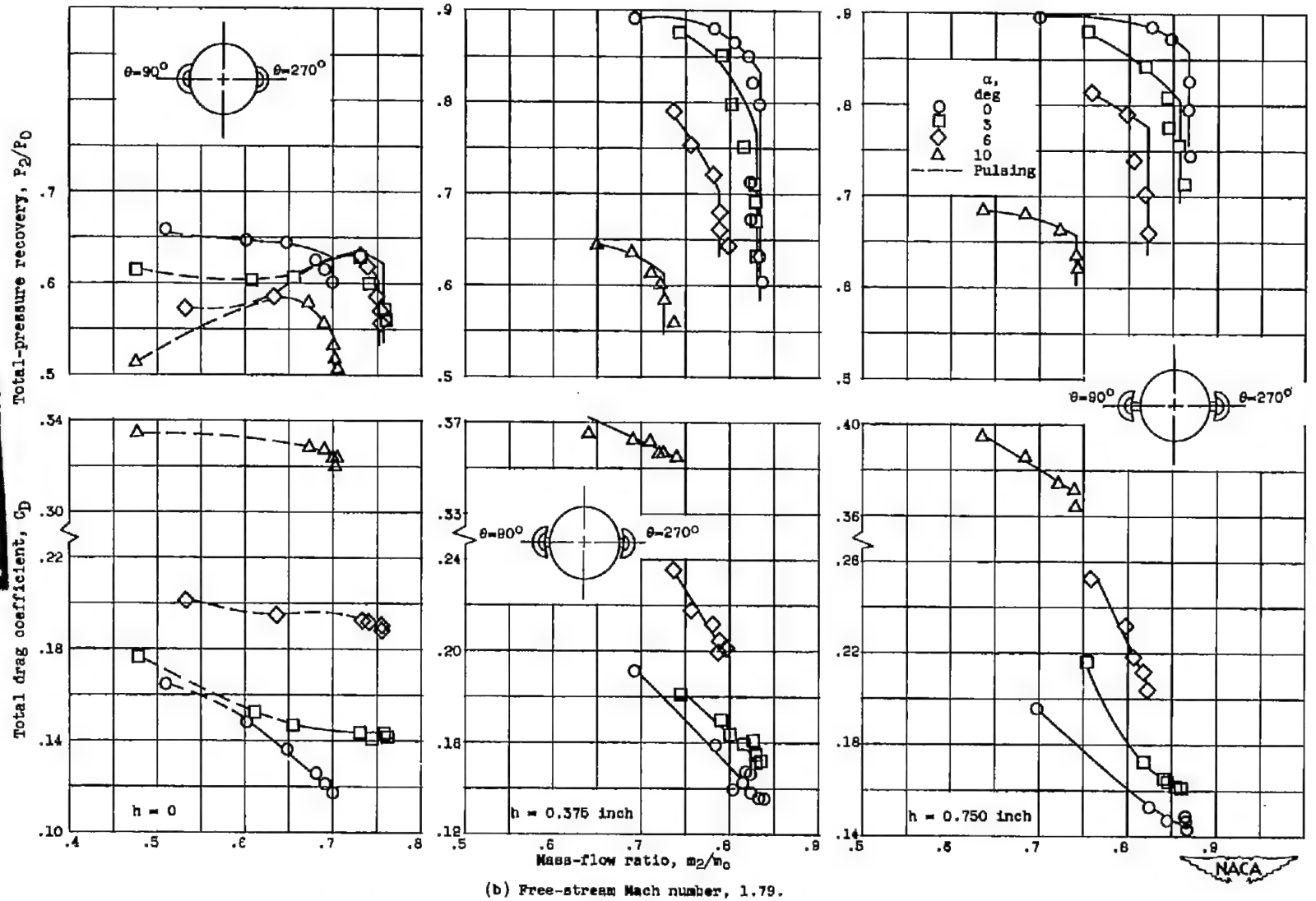

(b) Free-stream Mach number, 1.79.

Figure 9. - Continued. Angle of attack characteristics of RM-10 inlet configuration. θ = 90° and 270°.

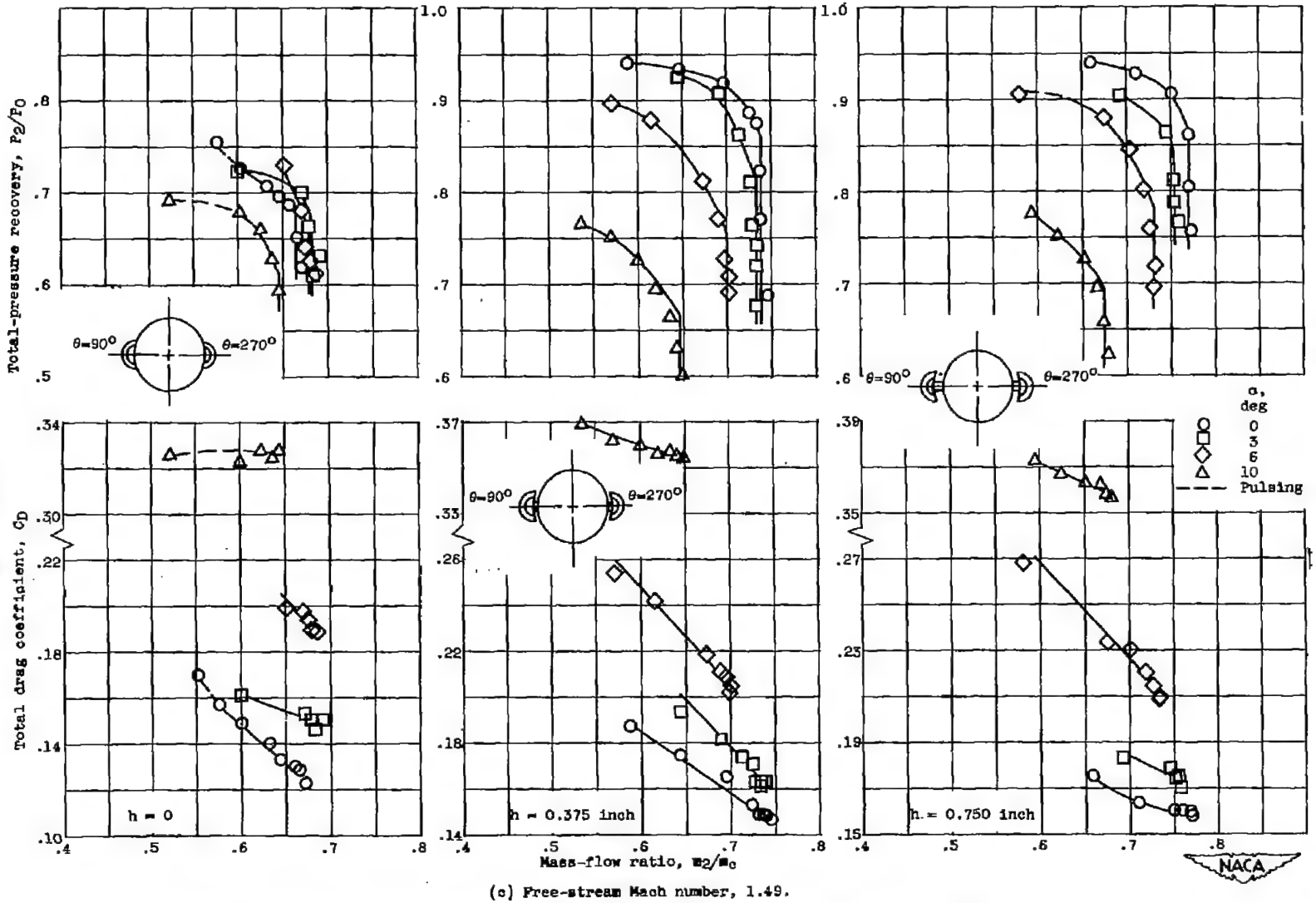

(c) Free-stream Mach number, 1.49.

Figure 9. - Concluded. Angle of attack characteristics of RM-10 inlet configuration. $\theta = 90^\circ$ and 270°.

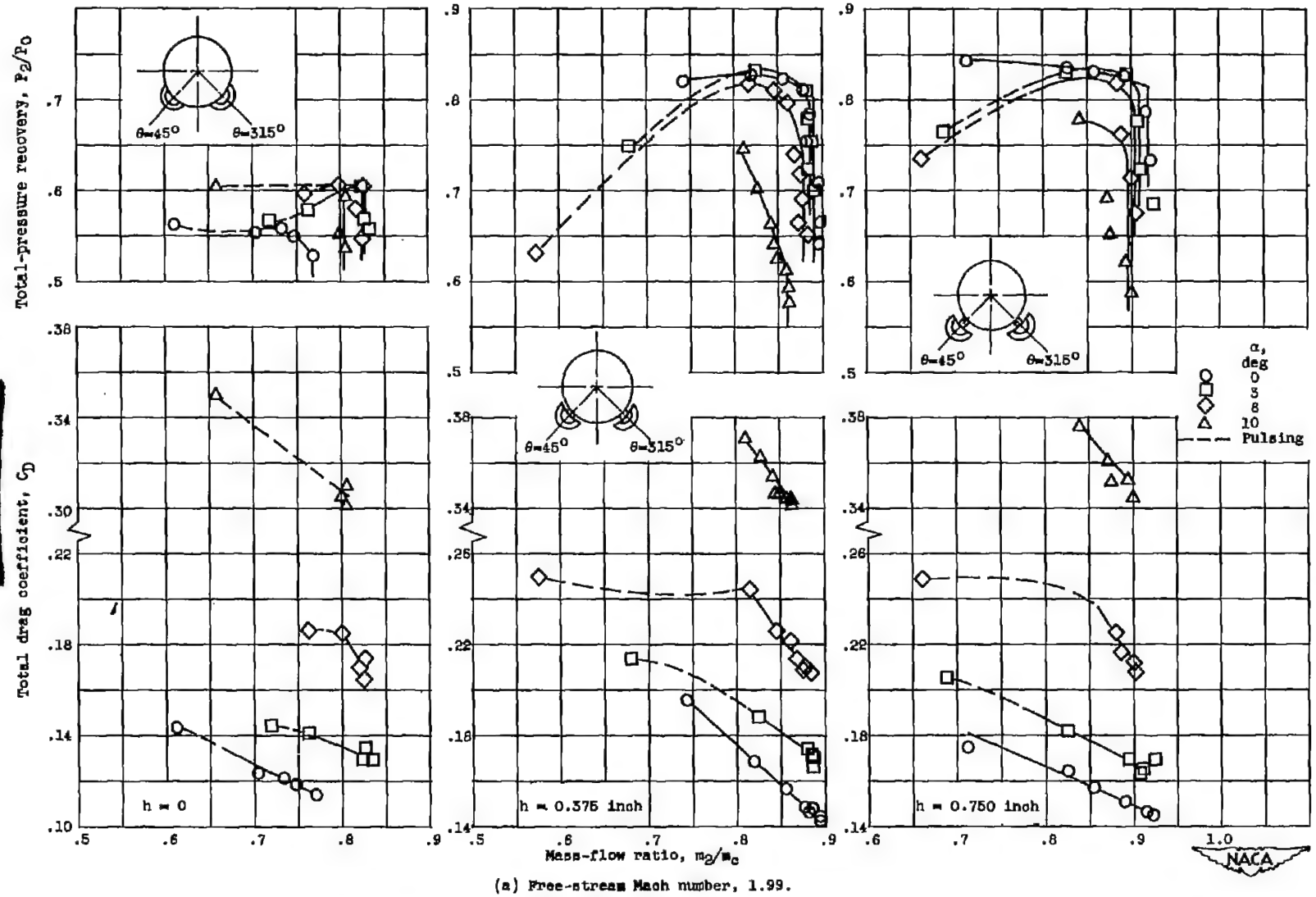

(a) Free-stream Mach number, 1.99.

Figure 10. - Angle of attack characteristics of RM-10 inlet configuration. $\theta = 45^\circ$ and 315°.

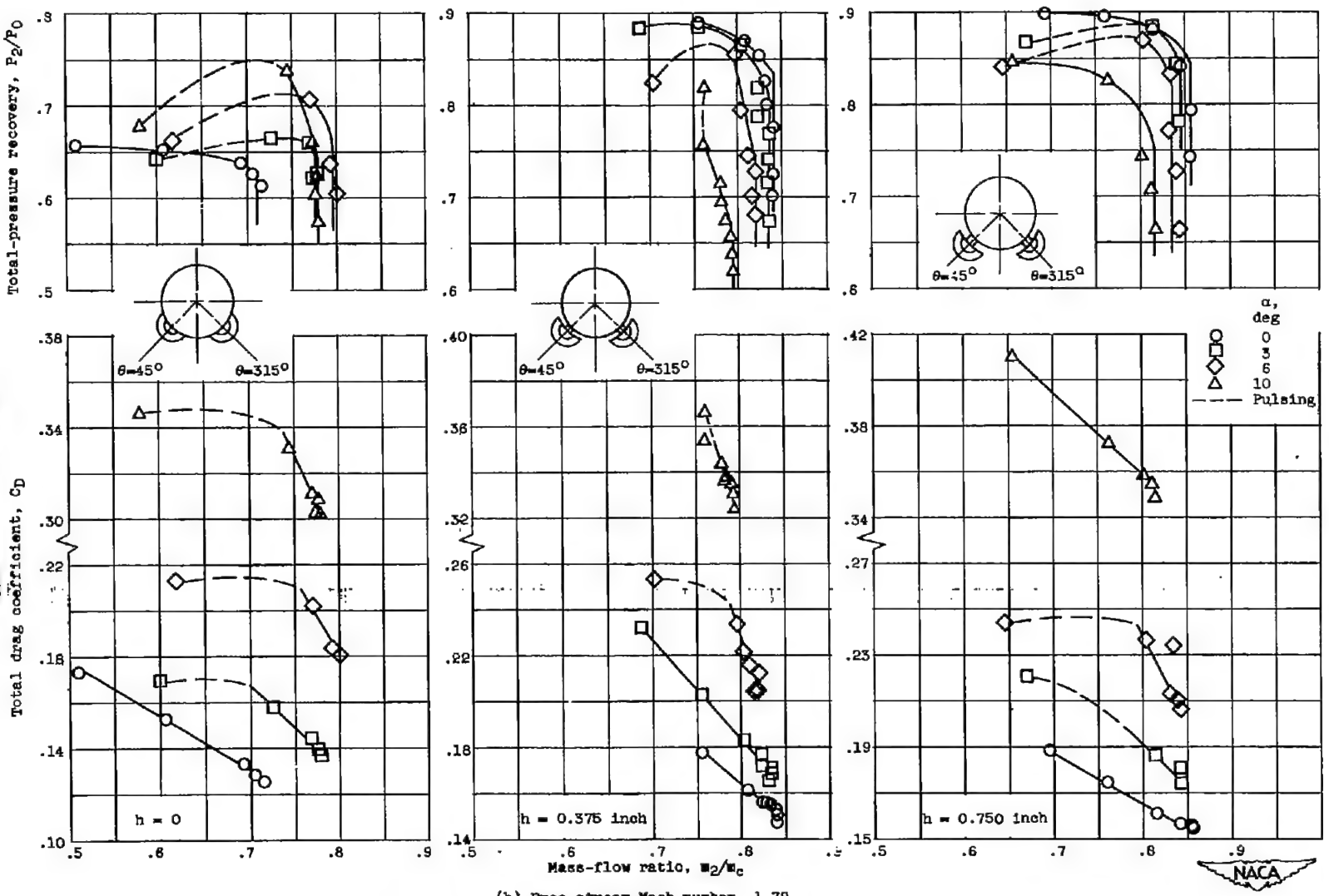

(b) Free-stream Mach number, 1.79.

Figure 10. - Continued. Angle of attack characteristics of RM-10 inlet configuration. θ = 45° and 315°.

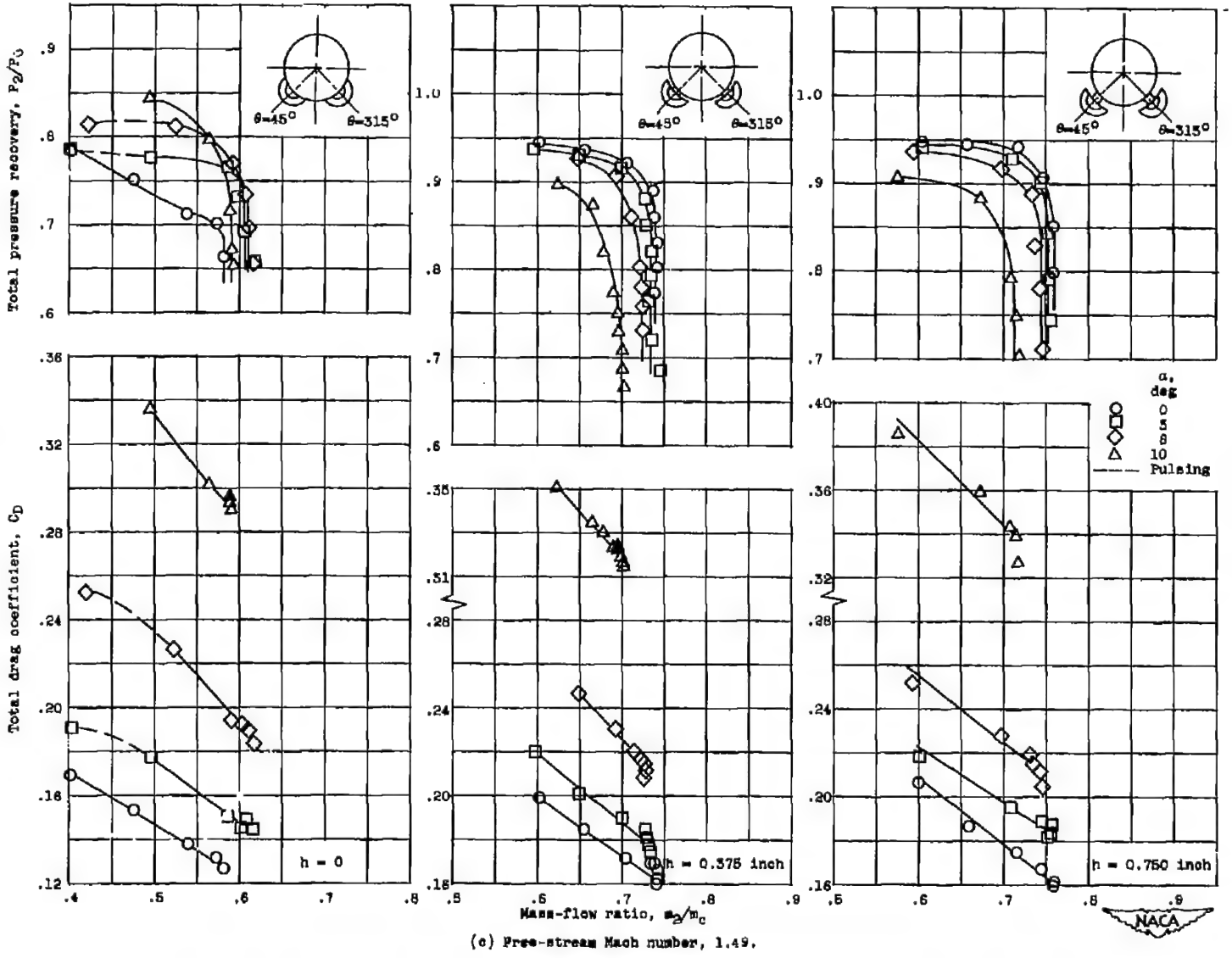

(c) Free-stream Mach number, 1.49.

Figure 10. - Concluded. Angle of attack characteristics of RM-10 inlet configuration. θ = 45° and 315°.

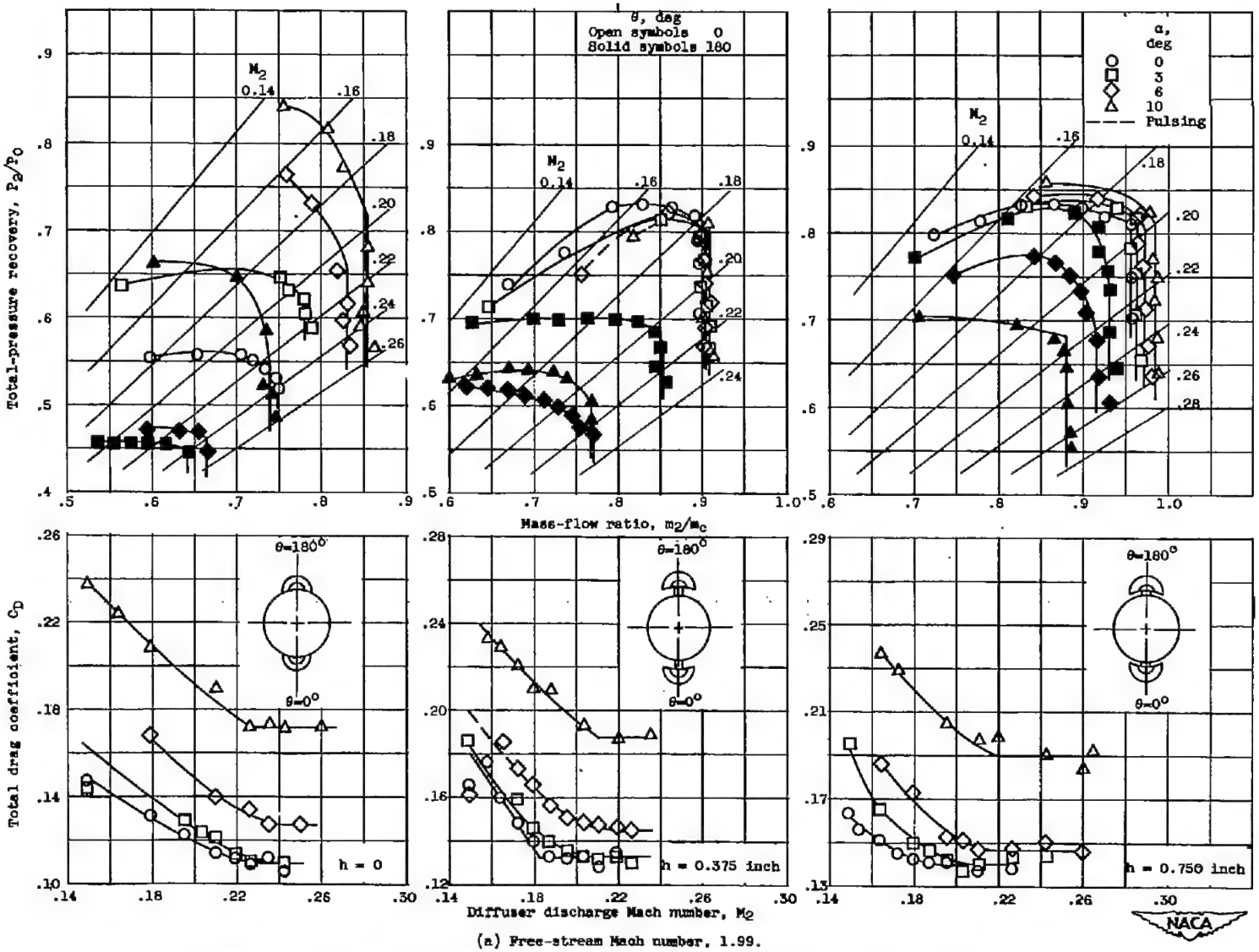

(a) Free-stream Mach number, 1.99.

Figure 11. - Angle of attack characteristics of RM-10 inlet configuration. $\theta = 0^\circ$ and 180°.

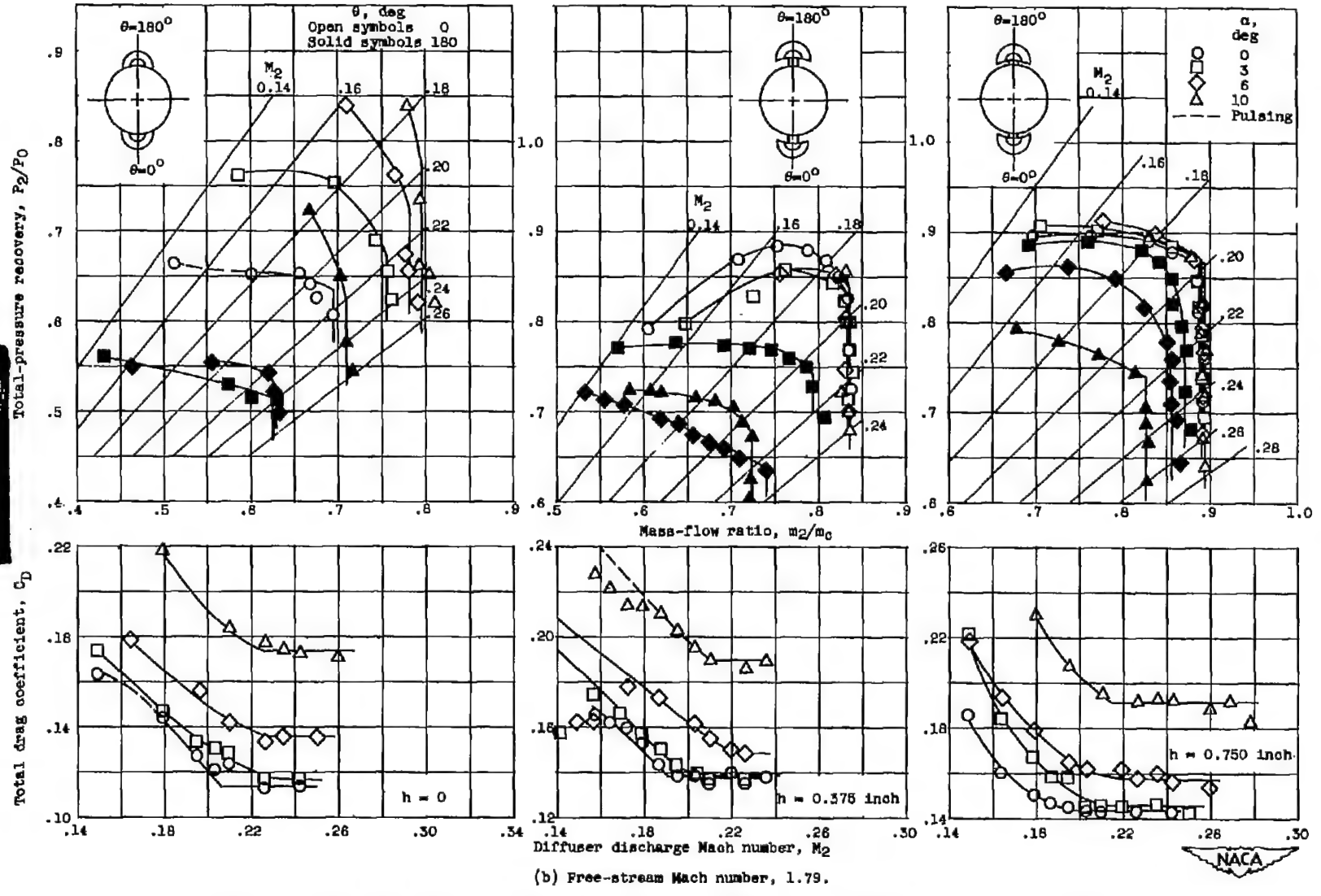

(b) Free-stream Mach number, 1.79.

Figure 11. - Continued. Angle of attack characteristics of RM-10 inlet configuration. $\theta = 0^{\circ}$ and 180°.

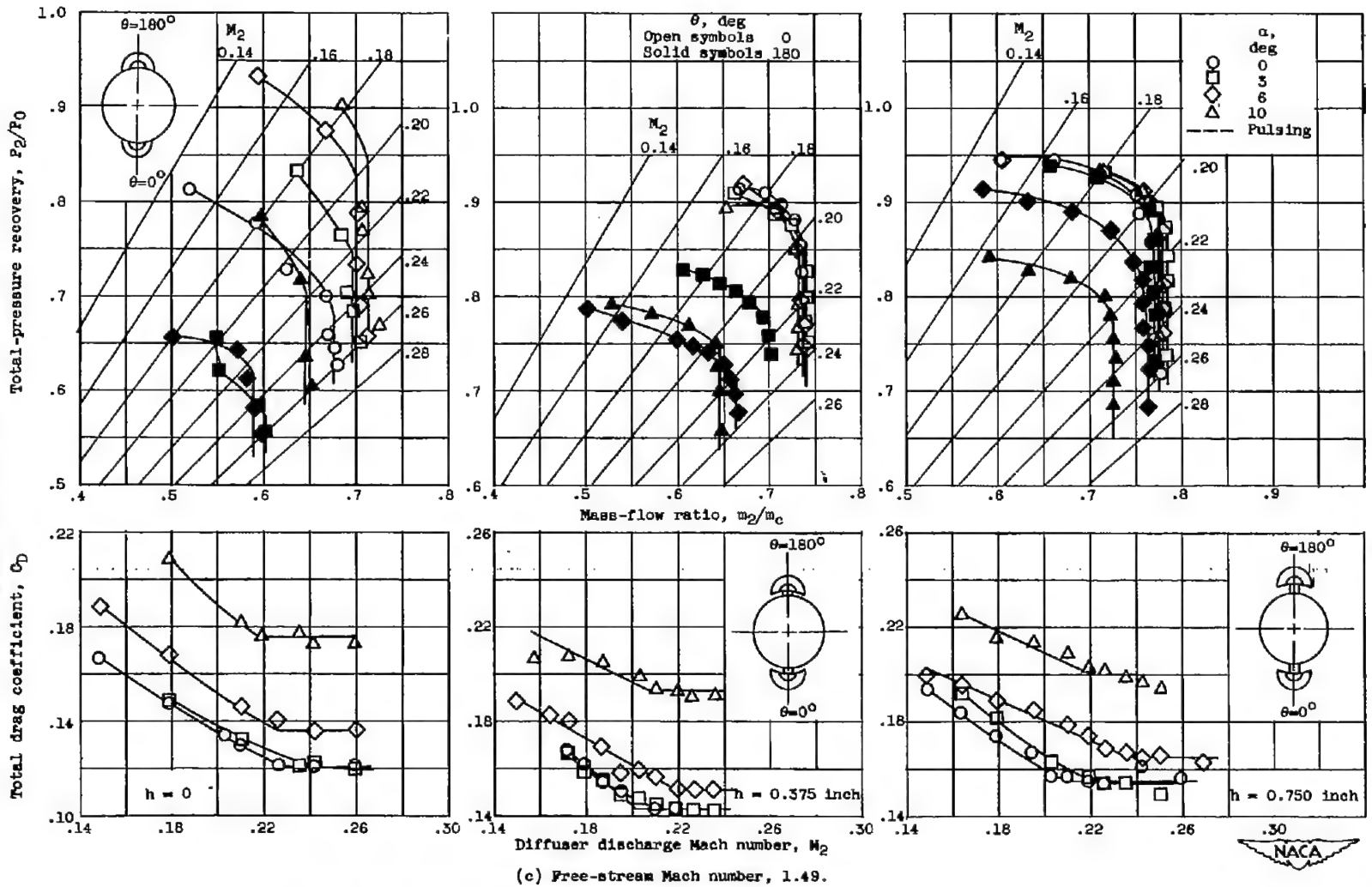

(c) Free-stream Mach number, 1.49.

Figure 11. - Concluded. Angle of attack characteristics of RM-10 inlet configuration. θ = 0° and 180°.

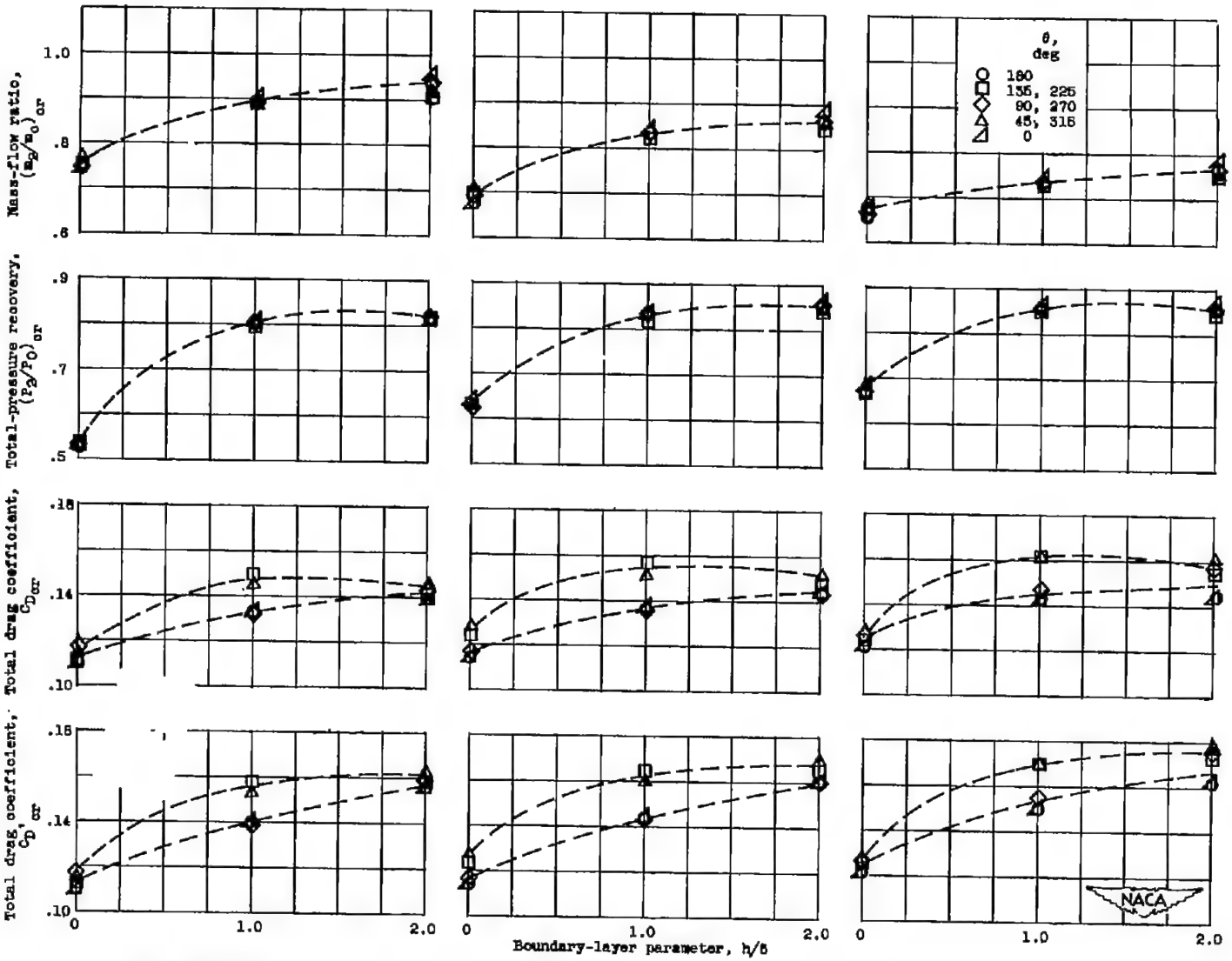

(a) Free-stream Mach number, 1.99. (b) Free-stream Mach number, 1.79. (c) Free-stream Mach number, 1.48.

Figure 12. - Effect of boundary-layer parameter on critical mass flows, pressure recoveries, and drag characteristics. $\alpha = 0°$.

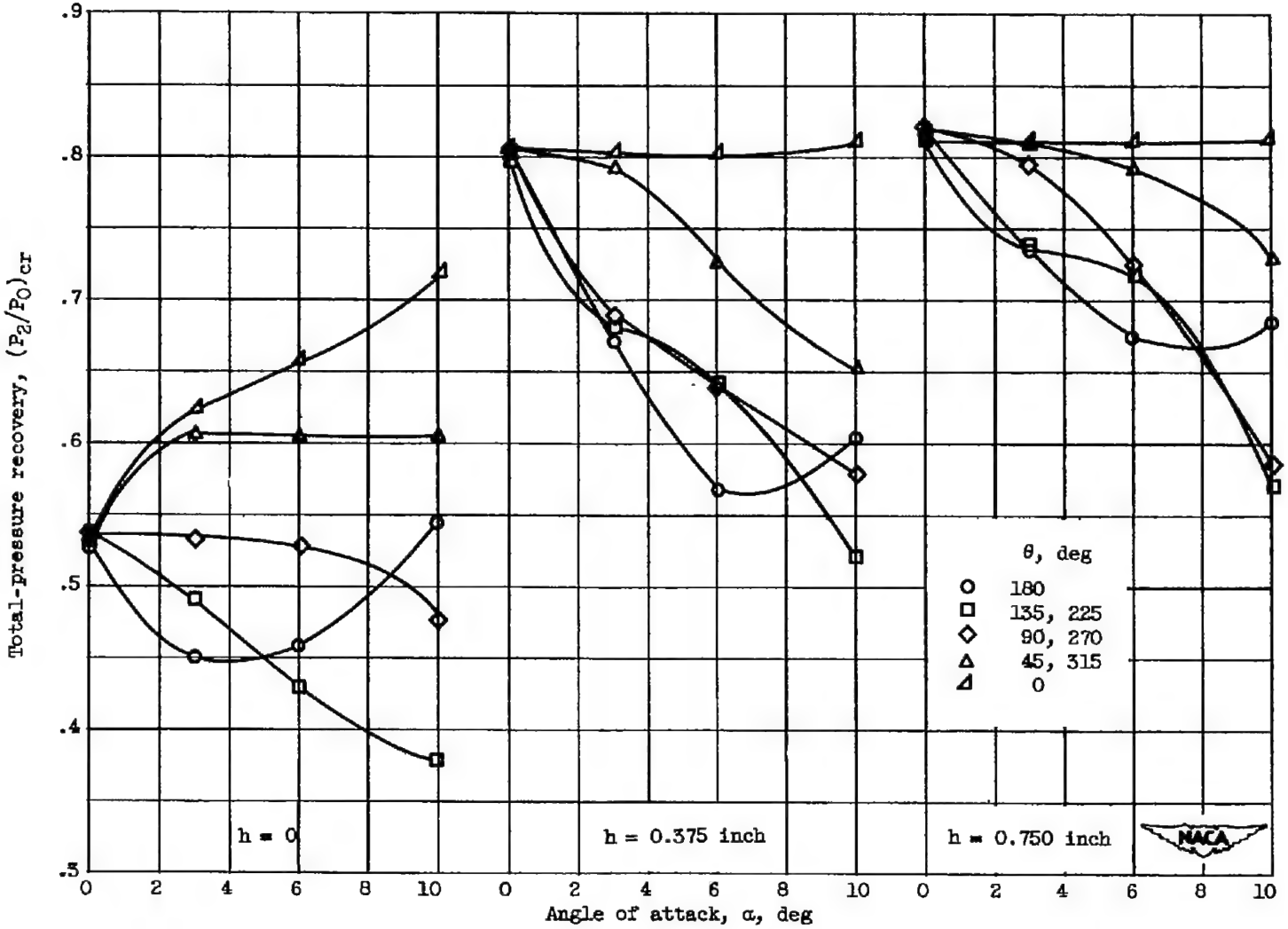

(a) Free-stream Mach number, 1.99.

Figure 13. - Effect of angle of attack on critical pressure recovery.

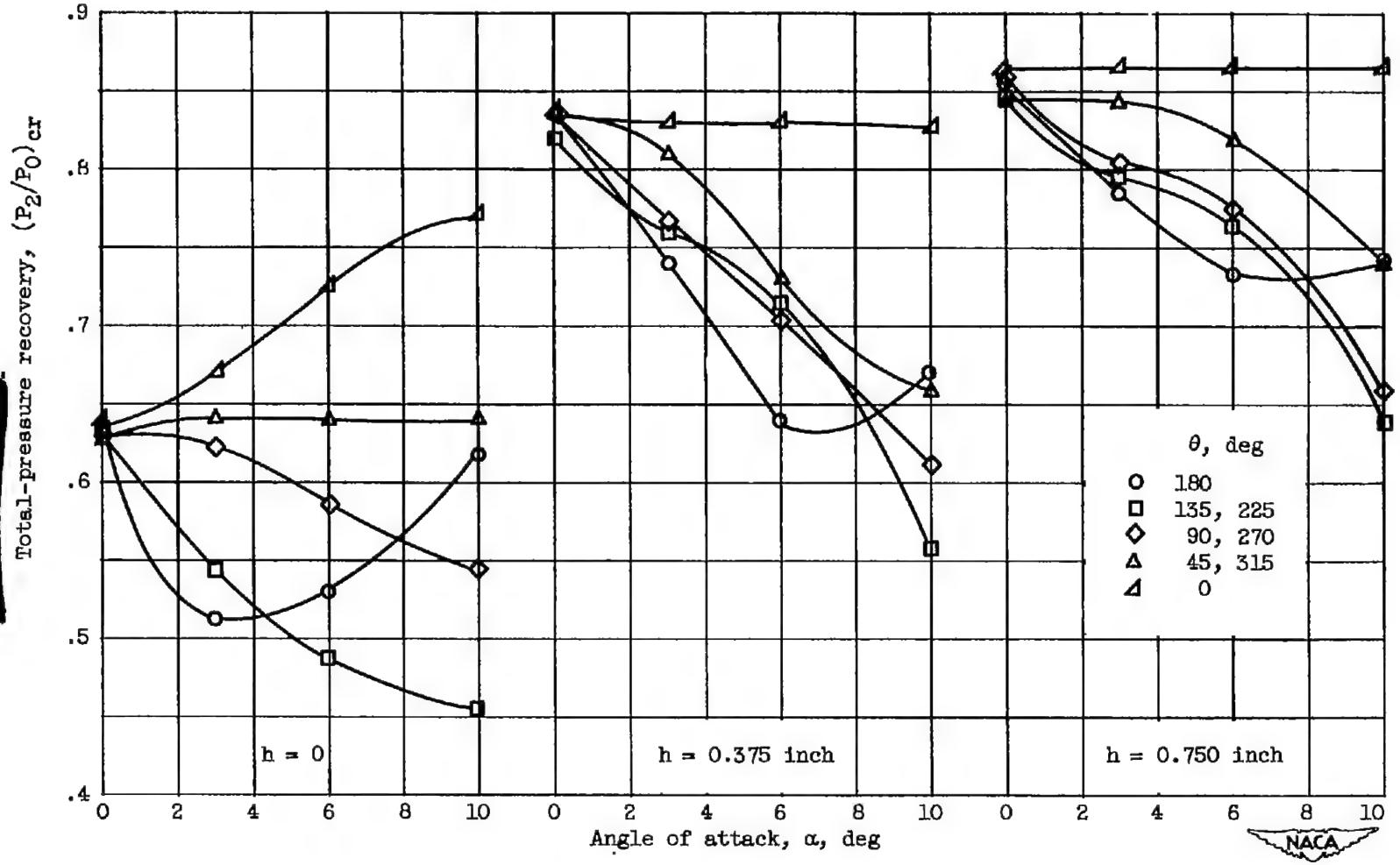

(b) Free-stream Mach number, 1.79.

Figure 13. - Continued. Effect of angle of attack on critical pressure recovery.

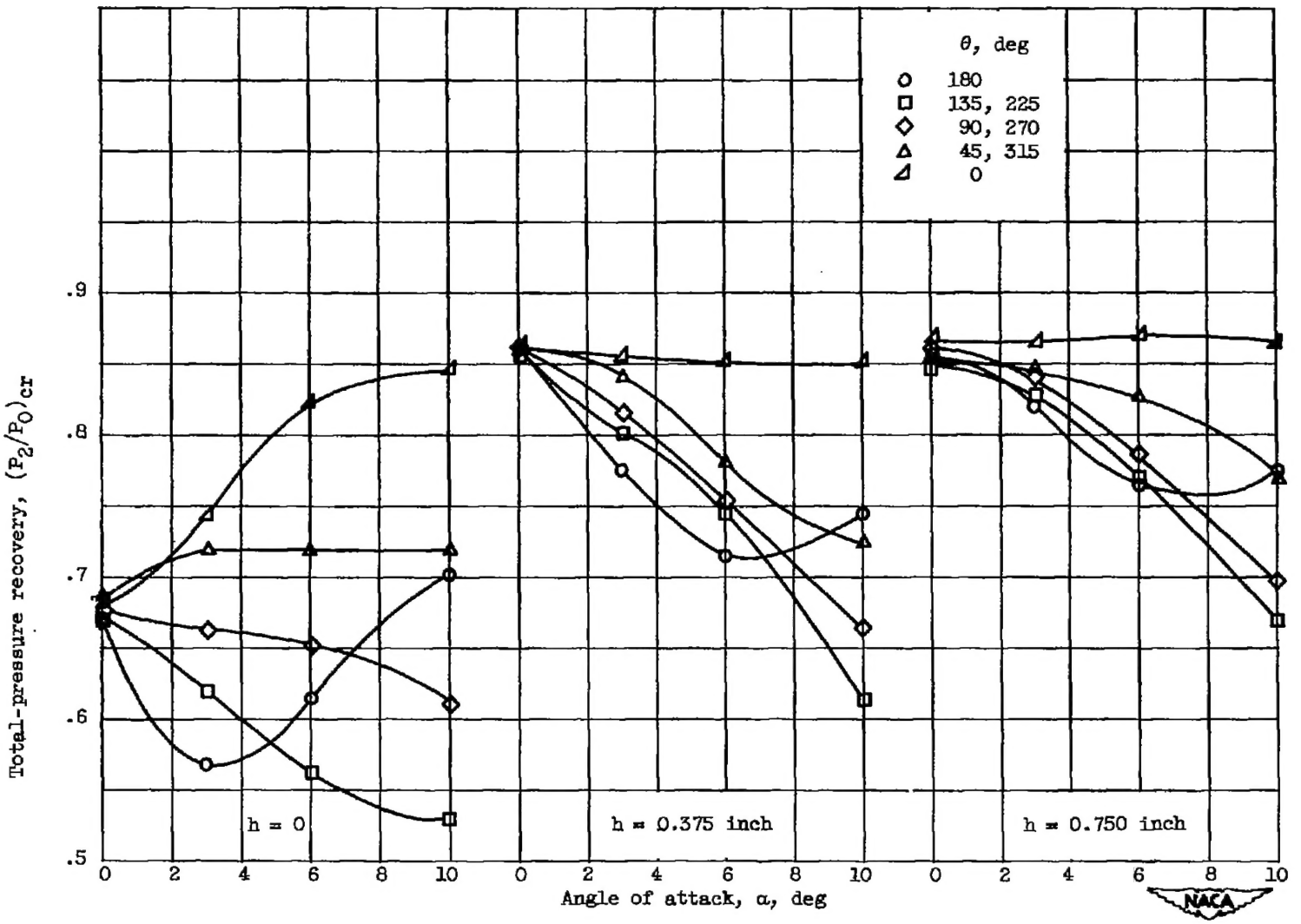

(c) Free-stream Mach number, 1.49.

Figure 13. - Concluded. Effect of angle of attack on critical pressure recovery.

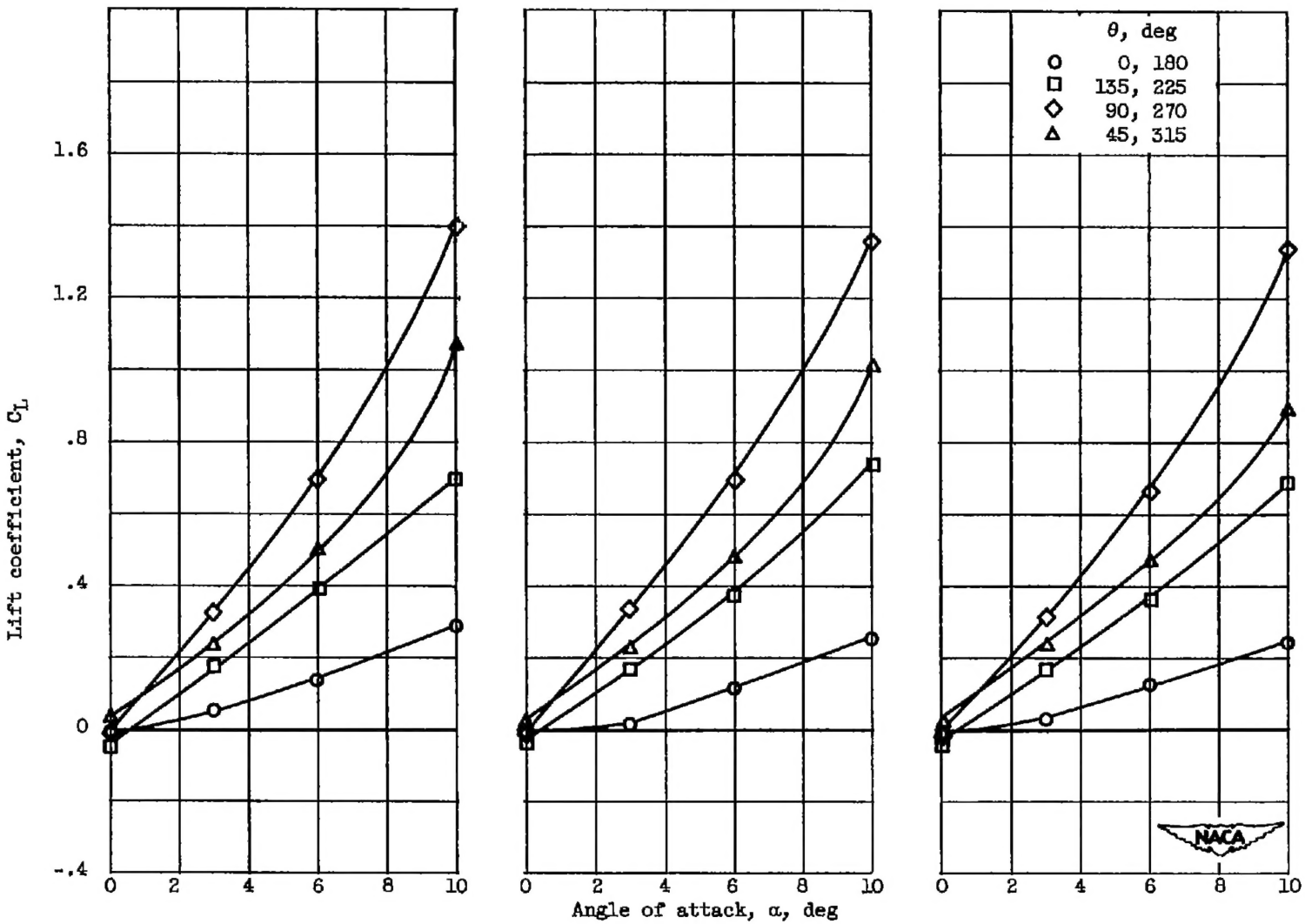

(a) Free-stream Mach number, 1.99. (b) Free-stream Mach number, 1.79. (c) Free-stream Mach number, 1.49.

Figure 14. - Effect of angle of attack on lift coefficient. h = 0.375 inch.

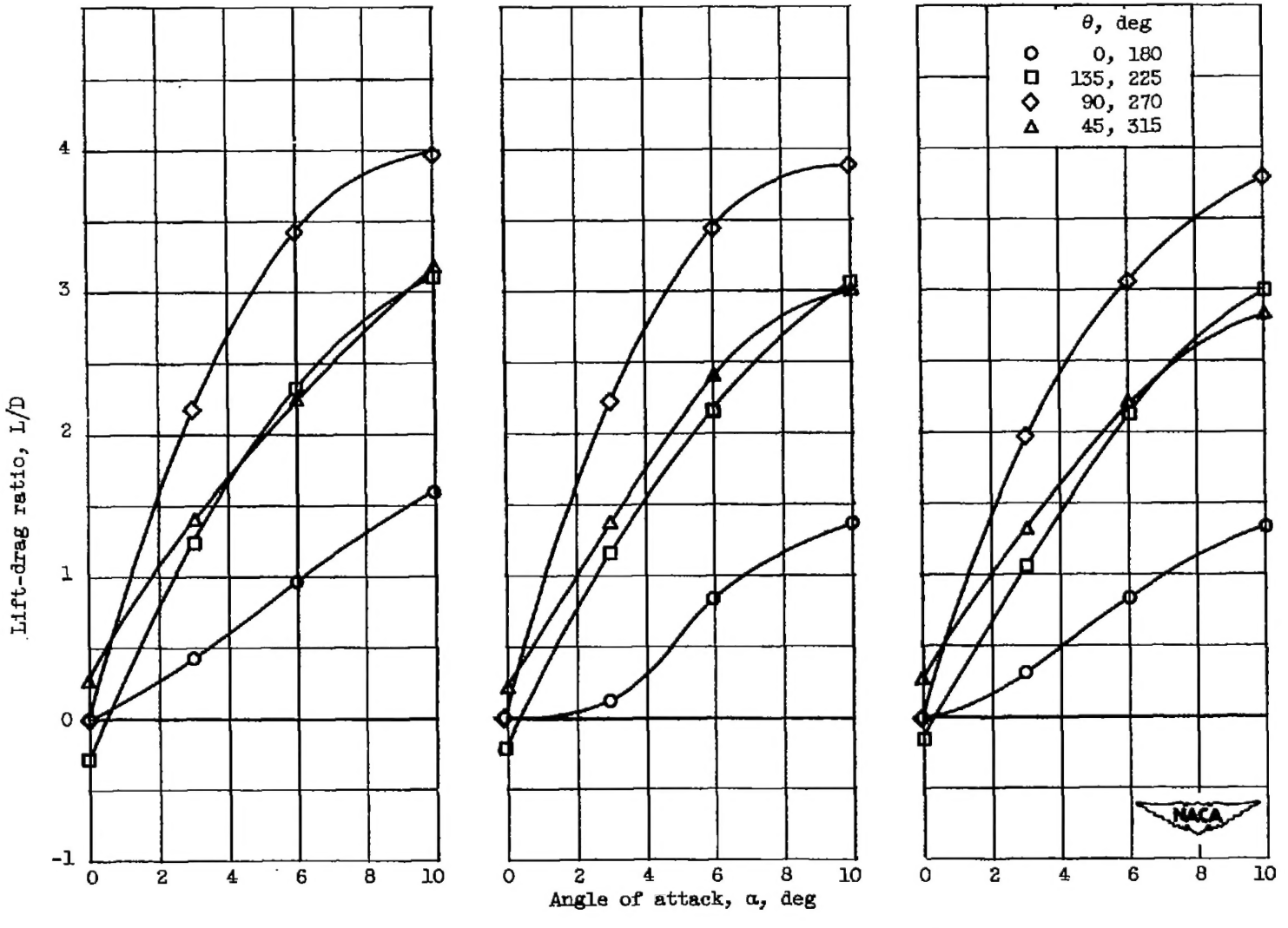

(a) Free-stream Mach number, 1.99. (b) Free-stream Mach number, 1.79. (c) Free-stream Mach number, 1.49.

Figure 15. - Effect of angle of attack on lift-drag ratio at critical mass flows. h = 0.375 inch.

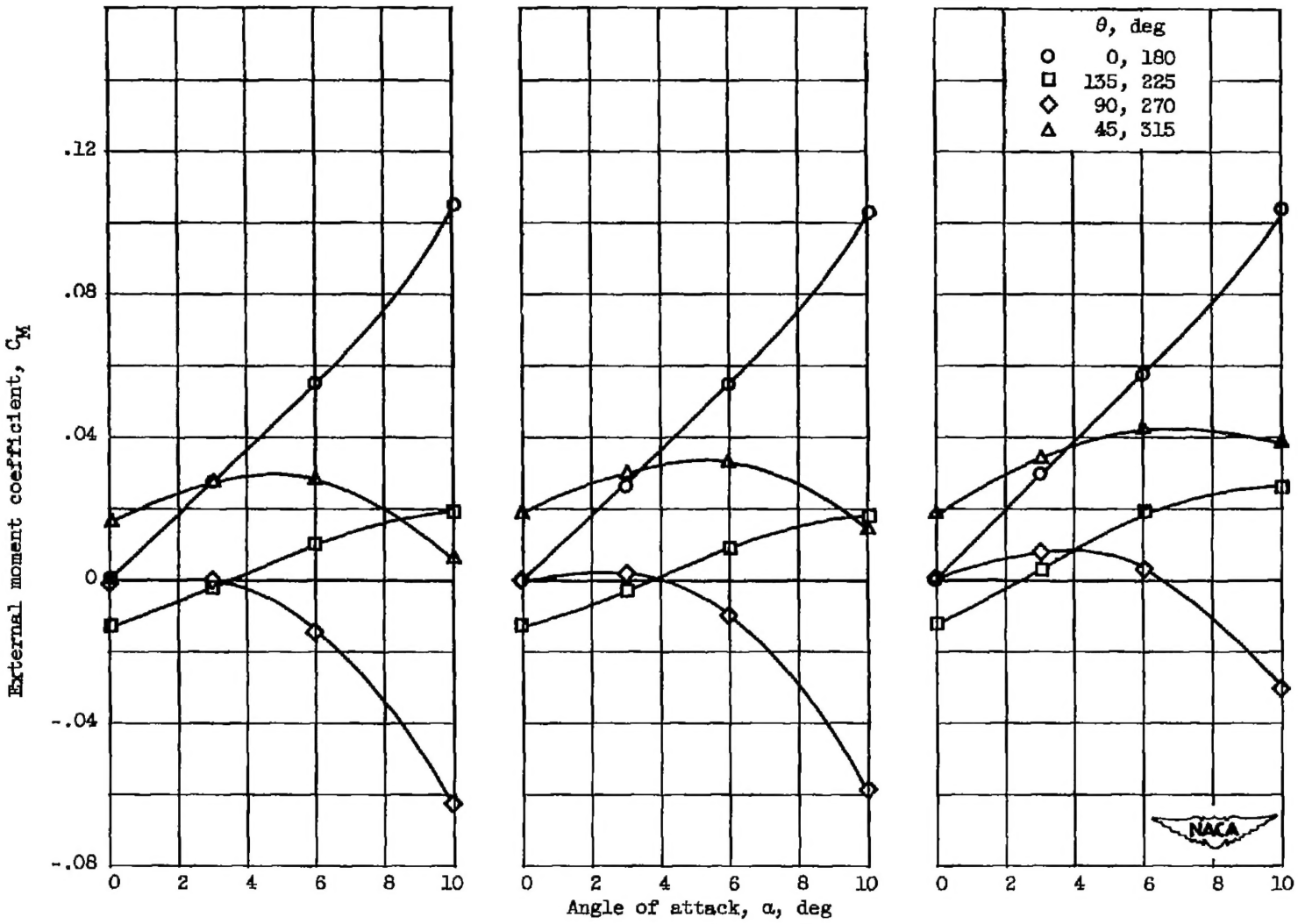

(a) Free-stream Mach number, 1.99. (b) Free-stream Mach number, 1.79. (c) Free-stream Mach number, 1.49.

Figure 16. - Effect of angle of attack on moment coefficient at critical mass flow ratios. h = 0.375 inch.